JOURNAL OF PETROLOGY | VOLUME 54 | NUMBER 9 | PAGES 1759–1792 | 2013 | doi:10.1093/petrology/egt030

Petrology and Geochemistry of the Crust–Mantle Boundary in a Nascent Arc, Massif du Sud Ophiolite, New Caledonia, SW Pacific

CASSIAN PIRARD[1,2]*, JÖRG HERMANN[1] AND HUGH ST. C. O'NEILL[1]

[1]RESEARCH SCHOOL OF EARTH SCIENCES, THE AUSTRALIAN NATIONAL UNIVERSITY, CANBERRA, ACT 0200, AUSTRALIA

[2]DEPARTMENT OF EARTH AND ENVIRONMENTAL SCIENCES, JAMES COOK UNIVERSITY, TOWNSVILLE, QLD 4811, AUSTRALIA

RECEIVED JULY 29, 2012; ACCEPTED MAY 2, 2013
ADVANCE ACCESS PUBLICATION MAY 30, 2013

The Massif du Sud ophiolite, New Caledonia, SW Pacific, is one of the largest exposed ultramafic bodies on Earth. The ophiolite consists of a mantle section of ultra-depleted tectonite harzburgite, overlain by a large dunite zone, which is separated by a transition zone from the gabbros at the top of the massif. Profiles through the stratigraphy of the mantle section show complex geochemical and petrological variations. The harzburgites are characterized by a high degree of partial melting and document a complex evolution from mantle exhumation towards a supra-subduction zone environment. Olivine and spinel compositions suggest that the harzburgites are residual after boninite-like melt extraction at 5–10 kbar. The lower dunite zone is analogous to the replacive dunite channels in the harzburgite, in that it is formed by pyroxene consumption. In contrast, the upper dunite zone has chemical and textural characteristics of cumulus olivine crystallized from primitive mafic melts. The upper dunite zone grades into a transition zone with pyroxenite cumulates that are intruded by gabbro sills. The crystallization sequence and mineral compositions indicate that pyroxenites and gabbros formed from hydrous, oxidized primitive basaltic magmas at ~1250°C and 2–4 kbar. Their geochemistry indicates that these parental melts are transitional between boninites and primitive arc magmas and carry a fore-arc basalt signature. The Massif du Sud therefore represents a crust–mantle section in a nascent arc. The cryptic transition between residual mantle rocks and crustal cumulates highlights the difficulty of estimating the thickness and average composition of an arc crust by seismic methods.

KEY WORDS: *New Caledonia ophiolite; arc crust; supra-subduction zone; crust–mantle boundary; dunite*

INTRODUCTION

Ophiolites are remnants of the oceanic crust and lithospheric mantle that have been accreted to the continental crust during tectonic events such as collision and obduction. Their relative accessibility allows the direct study of the rock types that form the oceanic lithosphere, making them an important source of information for understanding processes acting at mid-ocean ridges (MORs), marginal basins and subduction zones. The 1972 Penrose conference on ophiolites provided a new framework for the interpretation of ophiolites as sections of the oceanic lithosphere. In the following years, many ophiolites were interpreted as representing parts of former MOR spreading centres (Prinzhofer *et al.*, 1980; Ross *et al.*, 1980; Boudier & Coleman, 1981; Pallister & Hopson, 1981). However, in-depth study of classical ophiolites has led to a more nuanced view. From structural, tectonic, petrological and geochemical observations, many ophiolites are now interpreted to have passed through a supra-subduction zone (SSZ) environment, so that they potentially record magmatic events related to the subduction of an oceanic plate

*Corresponding author: E-mail: Cassian.pirard@jcu.edu.au

and the formation of volcanic arcs (Stern, 2004; Metcalf & Shervais, 2008).

Ophiolites such as the Oman, Troodos, Balkans and western US coastal ophiolites share features of both MOR and SSZ environments (Saccani & Photiades, 2004; Yamasaki *et al.*, 2006; Dilek *et al.*, 2007). Talkeetna and Kohistan have been interpreted as arc sections (Tahirkheli, 1979; Clift *et al.*, 2005), whereas other ophiolites appear to have the geochemical features of the mantle and crust of either fore-arc (Mirdita, Morishita *et al.*, 2011; Bay of Islands, Varfalvy *et al.*, 1997) or proto-arc (Ladakh, Chilas; Burg *et al.*, 1998; Dhuime *et al.*, 2007) settings.

In many of these large ophiolites the transition from mantle to crustal rocks is accessible, providing opportunities to ground-truth inferences from seismological observations on the constitution and thickness of the oceanic crust. Here there are some semantics that first need to be clarified. Seismological observations of the oceanic lithosphere reveal a discontinuity, the Mohorovičić discontinuity (henceforth 'Moho'), marking an increase in P- and S-wave velocities, which has traditionally been identified as marking the boundary between crust and mantle (e.g. White *et al.*, 1992). The increase in P-wave velocity is from $\sim$7 km s^{-1}, typical of gabbro, to $\sim$8 km s^{-1}, expected for olivine-dominated lithologies. From petrological, petrogenetic or geodynamic perspectives, however, it is useful to define the crust–mantle boundary in the oceanic lithosphere with reference to the origin of the lithologies: the mantle is the residual peridotite that remains after varying degrees of melt extraction, whereas the crustal rocks are the crystallization products from the extracted melts (Benn *et al.*, 1988; Miller & Christensen, 1994). This is because the amount of melt produced from upwelling mantle is the key observation in modeling the rifting at constructive plate margins to deduce the thermal structure of the mantle (McKenzie & Bickle, 1988). In general, the petrological boundary between crust and mantle so defined will not be coincident with the Moho, except in cases where the lowermost crystallization products of the extracted melt are gabbroic (*sensu lato*), and not the plagioclase-poor lithologies such as dunite, wehrlite and pyroxenite that might be expected in some tectonic settings.

The classic ophiolite sections listed above have been extensively studied with modern geochemical techniques, but other well-known examples, including the New Caledonia ophiolite, have not recently been reassessed. Geodynamic studies of the SW Pacific and research on the regional geology of the New Caledonia archipelago have suggested that the material of this ophiolite probably passed through a supra-subduction zone environment prior to its emplacement onto continental crust (Cluzel *et al.*, 2001, 2005). However, this hypothesis has not been tested by petrographic, petrological and geochemical studies. Despite being of considerable economic importance for Ni, Co and Cr resources, the ultramafic nappe, which covers 41% of the archipelago, has received little attention compared with other ophiolites of its size, such as those in the Sultanate of Oman. Petrotectonic and geochemical studies from three decades ago have been interpreted as suggesting an ocean-spreading environment with a paleoridge occurring along an east–west axis (Prinzhofer *et al.*, 1980). Early geochemical studies have shown that the New Caledonian peridotites are harzburgites that are highly depleted as the result of a high degree (>25%) of partial melting (Prinzhofer & Allègre, 1985). The resulting ultradepleted characteristics of the mantle rocks and the absence of primary clinopyroxene rule out many of the approaches usually used to study the geochemistry of mantle peridotites, although recent studies have been reported of the northern lherzolites (Ulrich *et al.*, 2010) and the crustal gabbros (Marchesi *et al.*, 2009).

The Massif du Sud ophiolite is the most depleted part of the ultramafic terrane of New Caledonia. Despite forming the largest continuous surface area of exposed mantle rocks in the world, it has never been subject to thorough petrological and geochemical investigations. The aim of this study is to provide an overview of the field characteristics, petrology and geochemistry of the southern part of this ultramafic nappe and to discuss their implications for the geological interpretation of the Massif du Sud ophiolite and the formation of oceanic arc crust in general. We provide evidence from the harzburgite and lower crustal gabbros that the New Caledonia lower crust and upper mantle section mainly formed in a supra-subduction zone environment. Special emphasis is placed on the dunite zone that occurs between the harzburgites and gabbros. We show that understanding the petrology and geochemistry of this zone is central to unravelling the position of the crust–mantle transition and the petrogenetic history of the ophiolite.

GEOLOGICAL FRAMEWORK

New Caledonia

The New Caledonia archipelago is located in the SW Pacific Ocean (Fig. 1a). Grande Terre forms almost 90% of the land area. Unlike most Pacific islands, which are relatively young and formed of Cenozoic volcanic rocks and carbonate platforms, Grande Terre is a complex assemblage of sedimentary, metamorphic and igneous terranes of varying age.

The island is divided into four super-terranes (Fig. 1b). The basement of Grande Terre records tectonic events that occurred at the end of the Palaeozoic and during the Mesozoic (ante-Senonian; >93·5 Ma), with accretionary complexes stacked onto the eastern margin of Gondwana (Aitchison *et al.*, 1995; Cluzel & Meffre, 2002). The opening of the Tasman Sea at the end of the Cretaceous period induced formation of several marginal basins to the east

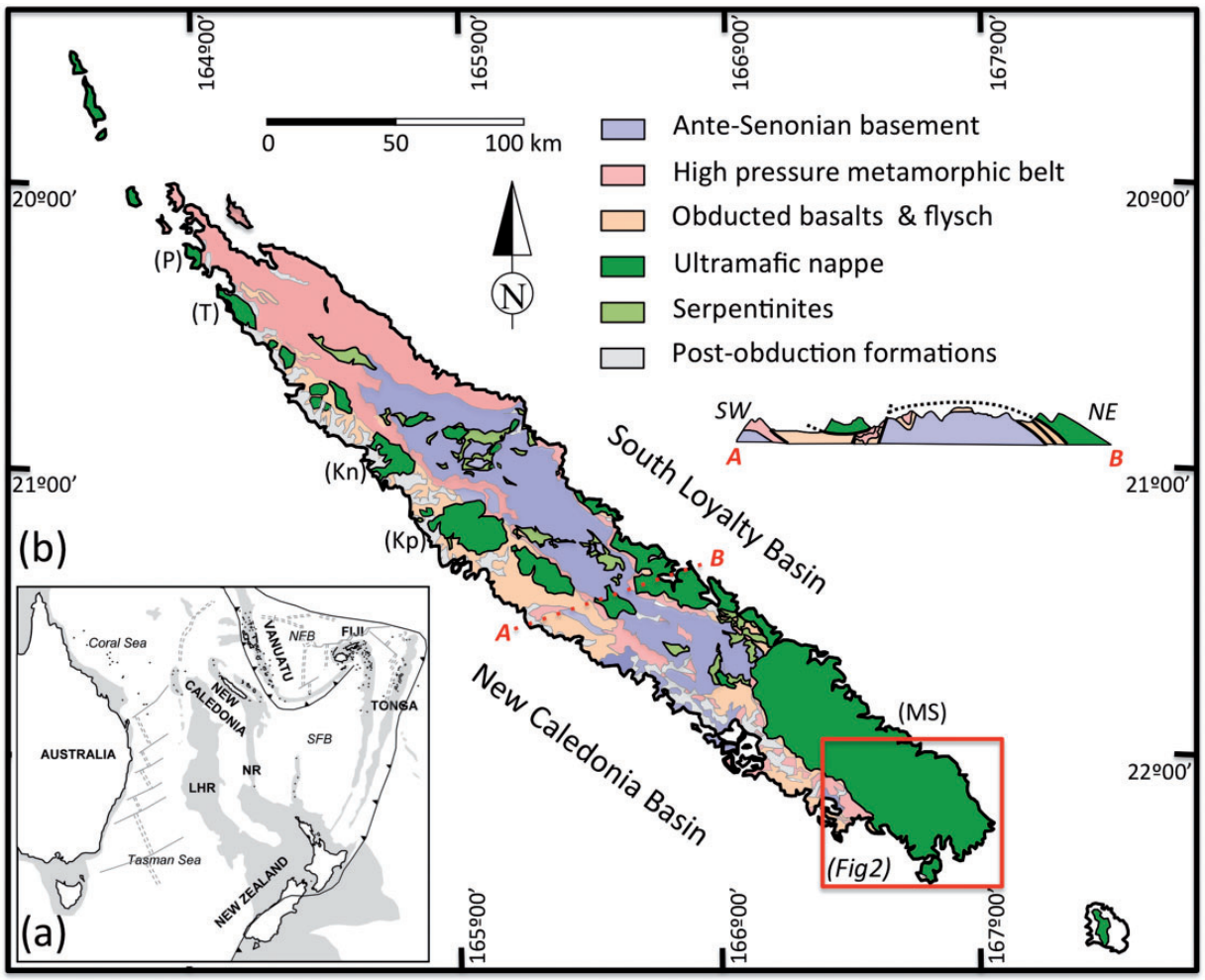

Fig. 1. (a) Present-day tectonic configuration of the SW Pacific showing the distribution of major tectonic features (Whattam *et al.*, 2008). LHR, Lord Howe Rise; NR, Norfolk Ridge; SFB, South Fiji Basin; NFB, North Fiji Basin. (b) Simplified geological map of New Caledonia showing the major super-terranes and the ultramafic terranes of Grande Terre (Paris, 1981; BRGM & DIMENC-SGNC, 2001). Locations: (P) Poum Massif; (T) Tiébaghi Massif; (Kn) Koniambo Massif; (Kp) Kopeto Massif; (MS) Massif du Sud.

of Gondwana and initiated several subduction zones to accommodate seafloor spreading (Schellart *et al.*, 2006). The formation of active margins led to the building of the second super-terrane of New Caledonia, from the subduction of the South Loyalty Basin during the early Tertiary. This super-terrane consists of a well-exposed high-pressure metamorphic sequence ranging from sub-blueschist- to eclogitic-facies conditions (55–44 Ma; Fitzherbert *et al.*, 2003; Spandler *et al.*, 2005; Potel *et al.*, 2006). Contemporaneous with high-pressure metamorphism was obduction of several oceanic terranes (flysch, basalts) onto the New Caledonia continental crust. This tectonic emplacement preceded subduction zone jamming, which occurred in the Late Eocene, coincident with obduction of the ultramafic terrane and associated gabbros (~32 Ma; Cluzel *et al.*, 1998, 2001). After these events, there was some minor magmatic activity at 27–24 Ma (Cluzel *et al.*, 2005) and the formation of sedimentary units by the erosion of earlier terranes. The present-day landscape is dominated by uplift and much surface alteration in a tropical environment (Sevin *et al.*, 2011).

Ultramafic terrane

The ultramafic terrane is a major feature of New Caledonian geology. It covers 8000 km^2 (41%) of Grande Terre and is thought to have once covered the whole island (Paris & Lille, 1977). The spatial distribution of this terrane includes several massifs on the west coast, some small nappes in the central chain and the Grand Massif Minier du Sud, which dominates the southern part of the island (Fig. 1b). Peridotites also occur on the smaller islands along the Norfolk Ridge, in altered outcrops on Belep Island, Yandé Island, Ile des Pins and Ouen Island. They have been identified in seismic studies as far as 300 km

north of Grande Terre (Guillon, 1975; Rodgers, 1975; Cassard *et al.*, 1981).

The ophiolite reaches a thickness between 1000 and 4000 m and is bounded at its base by a serpentinite sole related to the thrust fault responsible for the obduction. The ultramafic massifs have similar general characteristics and show an evolution in chemistry from north to south (Paris & Lille, 1977; Cassard *et al.*, 1981). With the exception of the northernmost massifs, the ophiolite comprises depleted harzburgite, locally ranging to dunite. In the Tiébaghi massif (Fig. 1b) a lherzolite zone is present, and further north the Poum massif largely consists of spinel and plagioclase lherzolite (Ulrich *et al.*, 2010).

The general lithostratigraphy shows that the highest levels of the ophiolite are exposed in the Massif du Sud where the crust–mantle transition can be identified, separating upper mantle peridotites from cumulate rocks and gabbros. The absence of a middle and upper oceanic crust in New Caledonia is thought to be due to either deep erosion or tectonic detachment (Cluzel *et al.*, 2001). About 8 km of additional rocks would have been present above the crust–mantle transition (Prinzhofer *et al.*, 1980). Within the Massif du Sud, the uppermost part of the ophiolite lies in the SW region of the ultramafic nappe (Fig. 2), whereas the deeper NE coast peridotite is considered to be still connected to the South Loyalty Basin oceanic crust (Prinzhofer *et al.*, 1980; Paris, 1981; Collot *et al.*, 1987).

Massif du Sud

The Massif du Sud is the only part of the ultramafic terrane that is of sufficient size to show kilometre-scale features, thus allowing depth-related variations to be established. The broad interpretation of this ultramafic–mafic sequence is relatively straightforward, as no major faults disrupt the nappe and the general structure is flat-lying, with local dips rarely exceeding 20° (Prinzhofer *et al.*, 1980). Mantle rocks are represented by harzburgite that occurs above the serpentinite sole, forming around 85% of the stratigraphic sequence (Fig. 3a). This harzburgite has a tectonite texture, in which foliation and lineation can be determined from the orientation of orthopyroxene porphyroclasts. Within the harzburgite, channels of dunite and pyroxenite are common. These features are more abundant in the higher part of the mantle section. In five areas, gabbronorite and olivine gabbro crop out (Figs 2a and 3), which represent the uppermost unit in the Massif du Sud. These gabbros clearly represent lower crustal rocks, and hence a continuous section from crust to mantle rocks is preserved. Between the large mass of mantle peridotites and crustal gabbros there is a large variety of rock types such as dunite with minor pyroxene, wehrlite, clinopyroxenite and websterite—called the transition zone (Dupuy *et al.*, 1981)—for which the origin is less clear. Dunite is the main lithology for over 500 m between the harzburgite and the pyroxenites of the transition zone (Fig. 2). Therefore the crust–mantle transition in the Massif du Sud ophiolite must occur in the 500 m to 1 km thick zone between the uppermost harzburgite and lowermost gabbro. Unless specified, we will use the term 'crust–mantle transition' for this zone.

PETROGRAPHY

Field observations and sampling

To determine the petrological and geochemical variations as a function of palaeo-depth within the oceanic, lithospheric mantle, we collected a series of ultramafic rocks along a stratigraphic transect in which unaltered rocks are exposed from the east coast (Yaté) to the centre (Montagne des Sources) of the ophiolite (Fig. 2b, Table 1). The pyroxenites and gabbros are exceptionally well preserved in the Montagne des Sources region. Detailed investigation was also undertaken in the north–south-trending Rivière des Pirogues valley, which cross-cuts the crust–mantle transition in several places from Montagne des Sources to Plum (Figs 2a and 3b). Additional samples were also collected on the NE coast, where the deepest level harzburgite was inferred to be exposed.

The sample collection covers harzburgite from different stratigraphic levels, the transition from harzburgite to dunite and a variety of lithologies from the transition zone and the gabbros. In addition to these main rock types, discordant features such as dykes or channels of dunite, pyroxenite and gabbro were sampled, as well as rare petrological features such as felsic intrusions, chromitites and hornblendites. These rocks will be the subjects of future publications.

Harzburgite

The lower and main part of the ophiolite is a depleted spinel-harzburgite of 2000–3000 m thickness, which forms 85% of the Massif du Sud (Figs 2a and 3a). Flow textures and shearing in the harzburgite classify the rock as a tectonite (Fig. 4a). This texture is present throughout the harzburgite but disappears locally where olivine–orthopyroxene segregations form a secondary layering parallel to the foliation (Fig. 4b). The general stratigraphy shows both an intensification of foliation and an increasing fraction of olivine up-section.

Most harzburgites contain primary Mg-rich olivine, which forms 75–85% of the rock. Olivine grain size can vary from 1 to >5 cm, but grains are always fractured and serpentinized and show many subgrain domains. Orthopyroxene forms 10–25% of the rock and occurs as large centimetre-sized elongated and kinked porphyroclasts (Fig. 4a). Cr-rich spinel (usually ~2% but rarely up to 10% modal) occurs mostly as xenomorphic holly-leaf shaped blebs growing between olivine and pyroxene grains. In some areas, 20% of the rock consists of porphyroclasts composed of a symplectite assemblage of pyroxene

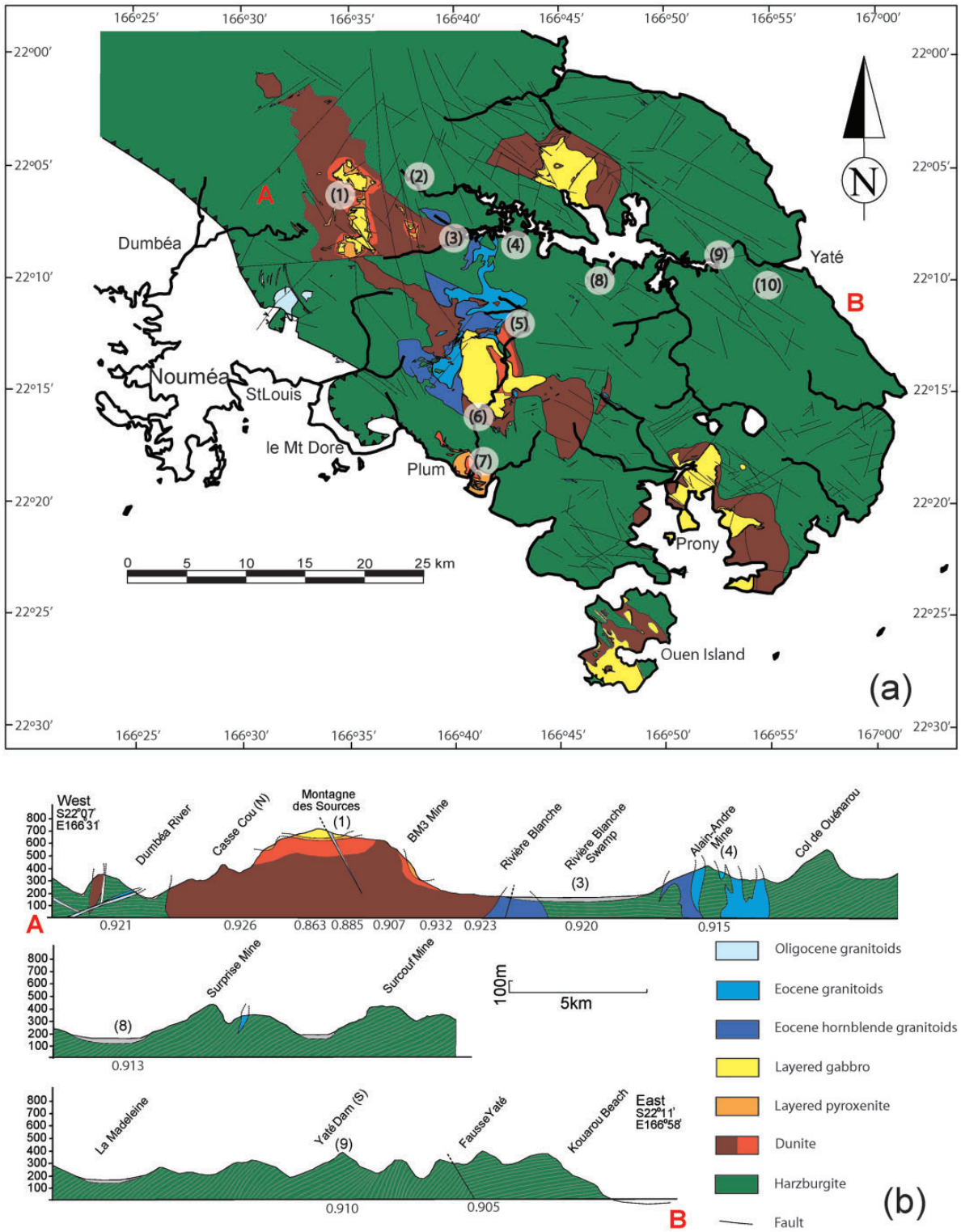

Fig. 2. (a) Simplified geological map of the southern part of the Massif du Sud. This figure is a compilation of data from BRGM maps, Prinzhofer *et al.* (1980) and our own field observations. Main sampling locations: (1) Montagne des Sources; (2) Rivière Bleue; (3) Rivière Blanche; (4) Parc de la Rivière Bleue–South road; (5) Rivière des Pirogues upstream; (6) Rivière des Pirogues downstream; (7) Baie des Pirogues; (8) Yaté road; (9) Yaté Dam; (10) Yaté Pass. (b) Cross-section (A–B) from Montagne des Sources and Dumbéa River (west) to Yaté (east) showing the stratigraphical sequence and the associated stratigraphic boundaries. Mg-number of olivine for specified areas along the transect is indicated on the *x*-axis.

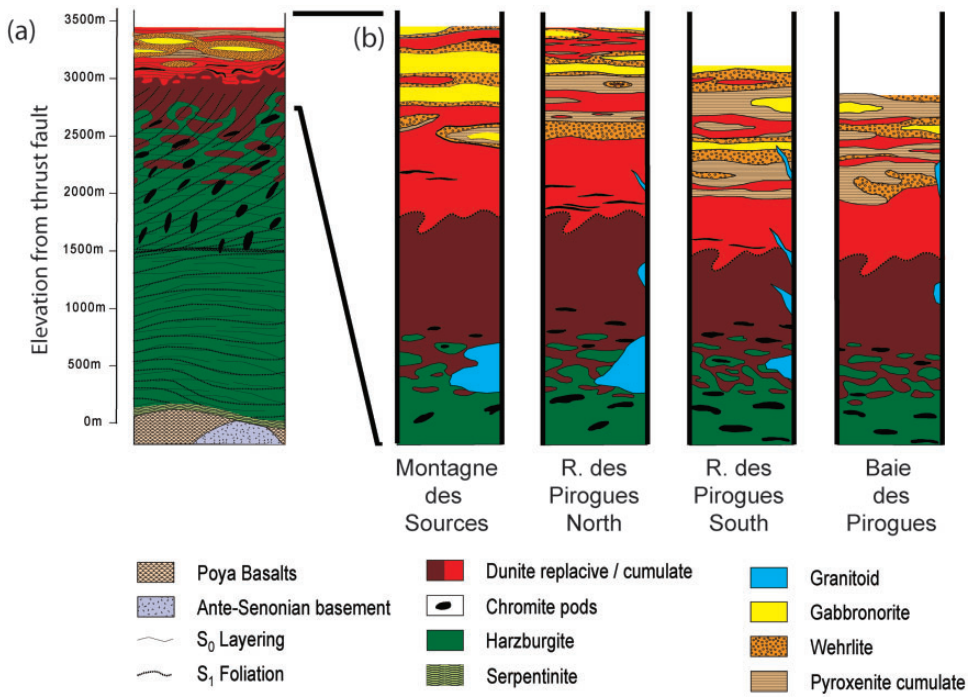

Fig. 3. (a) Schematic representation of the stratigraphy in the Massif du Sud [combined with textural data from Prinzhofer *et al.* (1980)]. (b) Details of the crust–mantle transition (from uppermost harzburgite to gabbros) for Montagne des Sources (1), Rivière des Pirogues north (5) and south (6) contacts and Baie des Pirogues (7) (see Fig. 2 for locations). An increasing amount of pyroxenite is seen from the north to the south.

and spinel (opx:cpx:sp = 0·55:0·15:0·30) (Figs 4a and 5). Clinopyroxene does not occur as a primary phase and is present only as minute exsolution laths in orthopyroxene, or as larger crystals in pyroxene + spinel symplectite clusters. In all cases, clinopyroxene modal concentration in harzburgite is less than 0·5%. Accessory primary phases are mainly sulfides and graphite (Augé *et al.*, 1999), which occur only in the lower part of the massif.

The base of the harzburgite section is defined by a sole of serpentinite resting on the previously accreted terranes of the Palaeozoic–Mesozoic basement. Away from this basal contact, and far from any major lineament through the massif, the harzburgite shows less serpentinization. Typically, around 30% of olivine is altered in the peridotite, although samples with less than 10% serpentinization can be found. In altered samples, serpentine (lizardite, antigorite) is occasionally associated with brucite, carbonates, magnetite and some Ni–Fe–Cu sulfides and alloys. Bastite, the field name given to serpentine-rich pseudomorphs after orthopyroxene, occurs in only the most altered samples.

Dunite

The modal content of orthopyroxene in the harzburgite decreases upwards, finally disappearing to define the dunite zone. The transition between the two rock units is not always obvious and is highly variable between locations. Some outcrops show a progressive trend from olivine-rich harzburgite to dunite, but in most places a sharp contact between orthopyroxene-poor harzburgite and dunite is observed (Fig. 4d). This transition occurs several times throughout the stratigraphy, suggesting that the harzburgite–dunite transition at the mapping scale is defined by where the dunite pods and layers, which are common in the upper harzburgite, eventually begin to greatly outnumber the host harzburgite and become the main lithology. The dunite zone is estimated to be between 400 and 600 m thick (Fig. 3) and can be separated into two distinct members.

The lower dunite zone mostly comprises olivine, which forms 90–95% (rarely up to 98%) of the rock (Fig. 4e). Chromite is the other primary phase and constitutes between 5 and 10 modal % (Fig. 5). Chromite appears as microsymplectite ribbons and clusters, and rare holly-leaf shaped grains (Fig. 5). The large symplectite and blebs of chromite that are present in the harzburgite are absent in the dunite zone. In some areas chromite can show monomineralic accumulations as layers and schlieren of chromitite (>50% spinel) (Fig. 4e). These rocks are different from the discordant to sub-concordant chromitite pods (Fig. 5) that occur in the lower part of the dunite zone and the upper harzburgite (Cassard *et al.*, 1981). The tectonite texture, which is clearly visible in the olivine-rich harzburgite and in the lowest dunite, becomes

Table 1: Location and description of samples

Sample name	Lithology	Texture	ol	opx	cpx	sp	plag	amph	Location	GPS latitude (S)	GPS longitude (E)
Yaté											
CY2	Harzburgite	tectonite	75	20		5			Yaté Pass (10)	22°09′58″	166°54′35″
YR2	Harzburgite	tectonite	76	20		4			Yaté Dam (9)	22°08′55″	166°53′02″
YA5	Harzburgite	tectonite	80	13		7			Yaté Dam (9)	22°08′55″	166°40′28″
R34	Harzburgite	tectonite	70	28		2			Yaté road (8)	22°9′39·7″	166°46′38·9″
Parc de la Rivière Bleue											
PRB34	Dunite	replacive	95			5			Southern lakeside road (4)	22°8′30·5″	166°42′10·2″
PRB49a	Gabbronorite	dyke		40	30		30		Rivière Blanche valley (3)	22°8′55″	166°37′19·5″
PRB49b	Olivine gabbronorite	dyke	10	40	30		20		Rivière Blanche valley (3)	22°8′55″	166°37′19·5″
PRB56	Olivine orthopyroxenite	cumulate	40	58		2			Rivière Blanche valley (3)	22°9′3·7″	166°38′45·3″
PRB58b	Harzburgite	tectonite	85	15					Rivière Bleue valley (2)	22°5′49·7″	166°38′16·7″
PRB61e	Harzburgite	tectonite	85	10		5			Rivière Bleue valley (2)	22°5′44″	166°38′15″
PRB61f	Harzburgite	tectonite	77	21		2			Rivière Bleue valley (2)	22°5′44″	166°38′15″
PRB72b	Dunite	tectonite	95	2		3			Rivière Bleue valley (2)	22°4′3″	166°37′05″
PRB75	Harzburgite	tectonite	83	13		4			Rivière Bleue valley (2)	22°4′1″	166°36′38″
Rivière des Pirogues											
RP31	Chromitite	cumulate	9		1	90			North (upstream) (5)	22°13′15·4″	166°42′53·5″
RP32	Dunite	cumulate	95		3	2			North (upstream) (5)	22°13′22″	166°42′52″
RP33	Wehrlite	cumulate	35	5	60				North (upstream) (5)	22°13′23″	166°42′52″
RP34	Harzburgite	cumulate	70	20	8	2			North (upstream) (5)	22°13′26″	166°42′51″
RP46	Amphibole gabbro	pod		10	65			25	South (downstream) (6)	22°14′52″	166°42′32″
RP51	Clinopyroxenite	cumulate	1	3	59	37			South (downstream) (6)	22°15′50″	166°42′28″
Montagne des Sources											
MDS32	Gabbro	dyke			50		50		Ridge track (1)	22°8′41·9″	166°35′16·6″
MDS34	Wehrlite	cumulate	80		15	2	3		Ridge track (1)	22°8′1·2″	166°36′17·9″
MDS36	Olivine gabbro	cumulate	60	1	25	14	10		Casse-Cou Mt track (1)	22°8′5″	166°36′20″
MDS37	Gabbronorite	cumulate	2	8	50		40		Casse-Cou Mt track (1)	22°8′6″	166°36′20″
MDS39	Wehrlite	cumulate	69		25	1	5		Casse-Cou Mt track (1)	22°7′53′	166°36′18″
MDS43	Dunite	cumulate	97			3			Casse-Cou Mt track (1)	22°8′34·2′	166°34′50·8″
MDS49	Dunite	cumulate	90	4		6			Cornice track (1)	22°9′1·9″	166°35′28·3″

macroscopically absent in the upper dunite zone owing to the lack of orthopyroxene as a marker. However, the microtexture of the lower dunite is still characterized by olivine aligned along a foliation. In the upper part of the dunite zone textures tend to be more isotropic and display rare layered characteristics (Fig. 4f). The size of olivine grains in the dunite zone remains relatively constant and they can be up to a decimetre in size. In the upper dunite zone, spinels occur as subidiomorphic grains (Fig. 5).

Transition zone

The crystallization of thick layers of orthopyroxene and clinopyroxene and the presence of interstitial minerals within dunite layers characterize the transition zone described by BRGM and Prinzhofer *et al.* (1980) (Fig. 6a and b). The top of the dunite zone is marked by the appearance of interstitial pyroxene or plagioclase between olivine grains. Rock types change frequently on a metre to 100 m scale (Fig. 3). Rocks in the transition zone have an obvious layering on an outcrop scale (Fig. 6c). Locally, cumulate features are also visible at smaller scales. In thin section, dunites are characterized by a matrix formed of rounded olivine and idiomorphic spinel grains (Fig. 5). Orthopyroxenes crystallize as relatively large, centimetre-size grains similar to, or larger than, olivine. In some areas, massive layers of pyroxenite or olivine wehrlite are also observed. Where olivine is subordinate, clinopyroxene ± plagioclase crystals are large, and tend to enclose olivine grains as

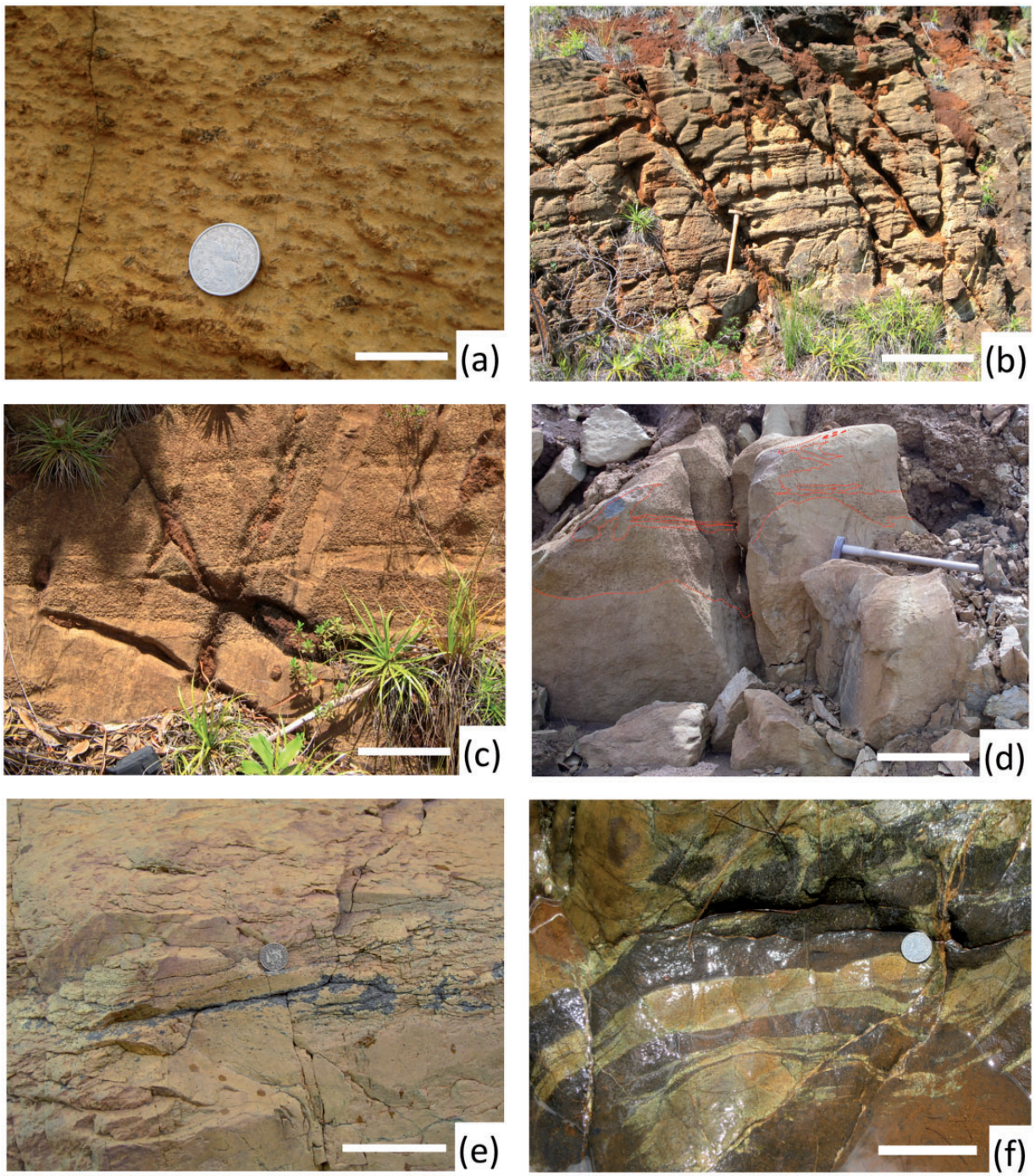

Fig. 4. Mantle rocks of the Massif du Sud ophiolite. (a) Deep harzburgite with a tectonite fabric. Olivine is altered and orange and hosts elongated orthopyroxene porphyroclasts. Some of the porphyroclasts are spinel–pyroxene symplectites. Yaté (9); scale bar 3 cm. (b) Harzburgite with very strong foliation giving an orthopyroxene-rich and olivine-rich layered appearance. GR2H mine (1); scale bar ~1 m. (c) Replacive dunite channels crosscutting harzburgite in the upper part of the ophiolite section and preserving some peridotite structures. Rivière Bleue (2); scale bar 0·2 m. (d) Dunite pod with complicated sharp contact with harzburgite (rugged surface). Pass of Prony [east of (7)]; scale bar ~0·5 m. (e) Lower dunite (orange) with chromite accumulation (dark brown). Rivière Bleue (2); scale bar 0·2 m. (f) Chromitite impregnation and schlieren (dark brown) in the dunite (orange) zone. Rivière des Pirogues (5); scale bar 10 cm.

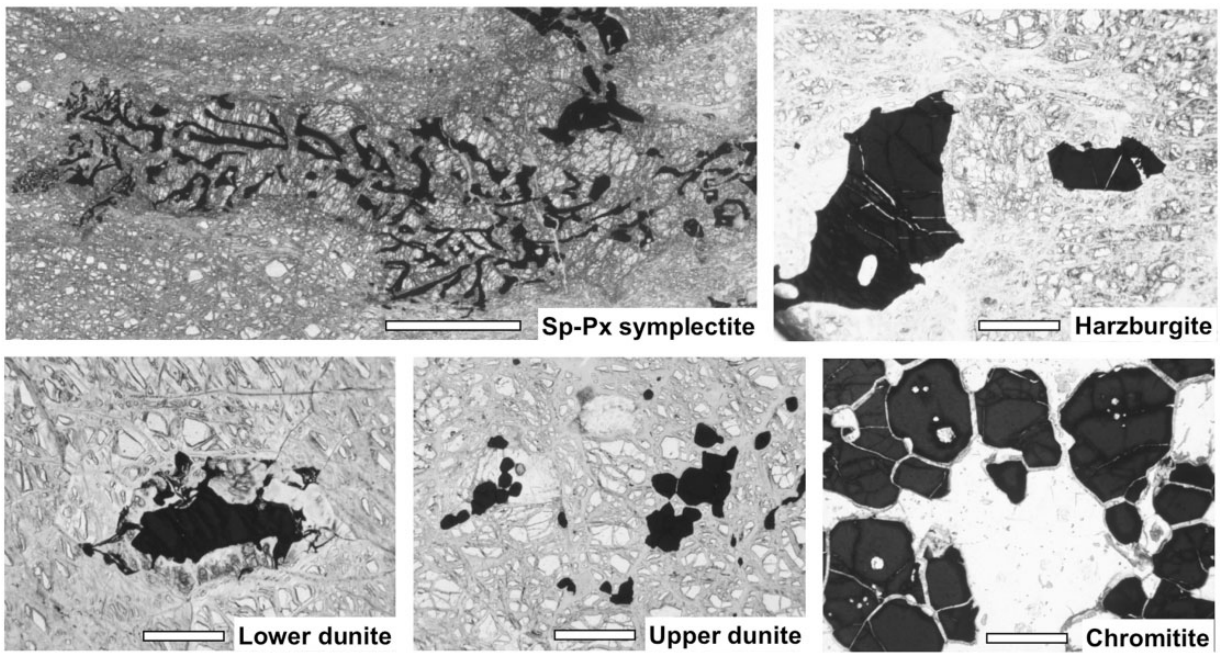

Fig. 5. Plane-polarized thin section photomicrographs of the texture of Cr-spinels within the various units of the Massif du Sud ophiolite. Clusters of chromite-symplectite intergrown with orthopyroxene and clinopyroxene, 50–2000 μm long, occur in the lower part of the ophiolite (Sp–Px symplectite; scale bar 500 μm). Harzburgite spinels are holly-leaf shaped grains, which occur between olivine and orthopyroxene crystals. In the lower dunite, chromite grains display an overgrowth of vermicular spinel. The upper dunite is formed by cumulus olivine containing (sub-)idiomorphic grains of Cr-poor spinel. Chromite in chromitite pods is in the form of large subiodiomorphic grains coexisting with olivine and containing inclusions of clinopyroxene or olivine. Scale bar 100 μm.

oikocrysts (Fig. 6e). Spinels are scarce in all these transitional rocks. Mapping showed that although pyroxene-bearing dunites are abundant in the lower levels, wehrlite and plagioclase-wehrlite are the most common rocks in the area surrounding the gabbros. This typical sequence has been interpreted as mafic cumulates by previous workers (Prinzhofer *et al.*, 1980) or as the result of melt impregnation processes (Marchesi *et al.*, 2009). Plagioclase-rich rocks such as anorthosite and troctolites are rare and form only marginal layers in the transition zone.

In the area surrounding the Montagne des Sources, the crust–mantle transition zone is broad and shows a sequence from dunite to gabbro characterized by an increasing modal component of clinopyroxene and plagioclase (Fig. 6c). In the Rivière des Pirogues, the transition zone can be accessed from both the north and the south. The transition is sharper than in the Montagne des Sources, with dunite in contact with pyroxenite layers (Fig. 3b). Thin sections of the dunite just below the crust–mantle transition show a very small amount of clinopyroxene and no evidence for plastic strain. This dunite is similar to the well-defined dunite layers that alternate with other ultramafic rocks of the transition zone. The transition zone in the Rivière des Pirogues is also considerably affected by the presence of chromitite bodies and late intrusions. The Baie des Pirogues massif, SW of the Rivière des Pirogues section (SE of Plum, Fig. 2), shows a transition zone that is more complex. Clinopyroxenites and websterites dominate the hill range, forming large sills or dykes in an olivine-rich rock (Fig. 3b). Amphibole is common in discordant pyroxenite bodies, providing evidence that some rocks crystallized from a hydrous mafic magma.

Gabbros

Gabbros are represented on the geological map as uniform and consistent bodies (Fig. 2) on top of the entire ultramafic sequence (Prinzhofer *et al.*, 1980; Marchesi *et al.*, 2009) (Fig. 3a). However, detailed mapping of the crustal sequences has revealed that the layered gabbros do not form a single continuous unit, but occur as several thick sills separated by wehrlitic or dunitic zones (Fig. 3b). Such features have been observed in other crustal sections of ophiolites, such as Oman, where a series of mafic sills intrude the ultramafic rocks (Smewing, 1981; Boudier *et al.*, 1996). Two out of the five gabbroic bodies in the Massif du Sud were sampled for this study, specifically those at Montagne des Sources and Rivière des Pirogues. At both localities, there is generally a succession of gabbro lenses, several metres thick, with diffuse boundaries evolving into plagioclase-bearing wehrlite. Layering is visible in some places (Fig. 6d) but is not widespread and not evident in all outcrops or in thin section.

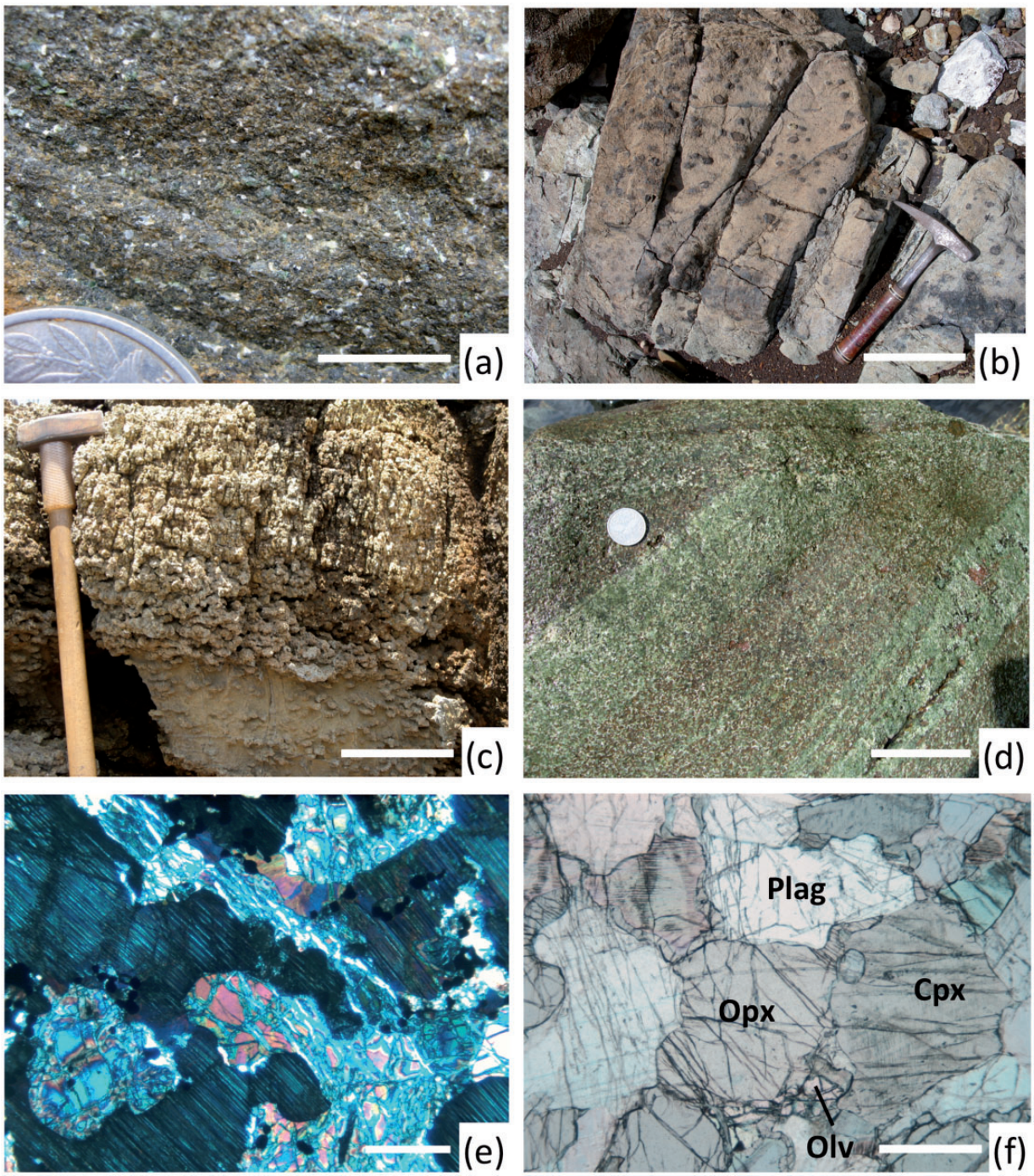

Fig. 6. Crustal rocks of the Massif du Sud ophiolite. (a) Dunite with cumulus olivine (dark brown) containing interstitial clinopyroxene (green) and plagioclase (white). Montagne des Sources (1); scale bar 1 cm. (b) Dunite with scattered clinopyroxene forming large poikilitic crystals within the dunite. Rivière des Pirogues (5); scale bar 20 cm. (c) Progressive impregnation of dunite by clinopyroxene (bottom) to clinopyroxenite with accessory olivine (top). Montagne des Sources (1); scale bar 10 cm. (d) Cyclic layering in an olivine gabbro displaying alternation between gabbronorite (green–white) and olivine-rich gabbro (brownish). Discordant layering (top) is related to a magma stoping event in the oceanic crust. Rivière Bleue (2); scale bar 0·1 m. (e) Poikilitic texture under crossed polars of a wehrlite layer surrounding a gabbro sill. Olivine is visible as isolated grains within a large clinopyroxene (in extinction orientation). Montagne des Sources (1); scale bar 100 μm. (f) Coarse-grained gabbronorite with abundant orthopyroxene and minute olivine grains in plane-polarized light. Montagne des Sources (1); scale bar 250 μm.

The gabbroic rocks all contain orthopyroxene (5–20%) and are thus gabbronorites. They have a range of composition from mela- to leuco-gabbro. Olivine grains are generally present as an accessory phase, forming rounded and fractured grains in a matrix of large crystals of plagioclase, clinopyroxene and orthopyroxene (Fig. 6f). Al–Cr spinels are rarely present. Alteration phases include iddingsite mixtures in olivine grains and hydrogrossular on the rim of plagioclase. Uralitization and saussuritization are frequent in some areas and form tremolite, nephrite, epidote and smaragdite.

Basalt at the top of Montagne des Sources was previously interpreted by Dupuy *et al.* (1981) as part of the ophiolitic sequence. However, field observations show that such basaltic outcrops can occur in the dunite zone or in the harzburgite and are likely to be related to magmatism postdating the obduction of the ophiolite.

ANALYTICAL TECHNIQUES

Chemical analyses of major elements in minerals were performed on polished thin sections with a CAMECA SX100 electron microprobe at RSES, ANU operating in wavelength-dispersive mode. Acceleration voltage and beam current were 15 kV and 20 nA, with a focused beam diameter of 1 μm. Counting times per element ranged from 20 to 50 s depending on the concentration and time optimization for each spectrometer. Several analyses on each phase were performed to obtain representative compositions and core–rim analyses were carried out to assess zoning patterns. Standards were natural (Mg, Si, Na, Al, K, Cr, Mn, Fe) and synthetic minerals (Ca, Ti) as well as pure metals (V, Co, Ni), which were all determined on the Kα emission peak. In-house mineral standards were used as secondary standards.

We did not undertake bulk-rock geochemical analysis of ultramafic rock samples owing to their depleted character and the presence of minor serpentinization in all samples. Instead we performed *in situ* analysis of the primary phases olivine, orthopyroxene and spinel. In the transition zone and mafic rocks, trace element data were also collected on clinopyroxene and plagioclase.

Trace elements in minerals were analysed by laser ablation inductively coupled plasma mass spectrometry (LA-ICP-MS) at RSES, ANU using a pulsed 193 nm ArF Excimer laser with 3–7 mJ of output energy reaching the sample at a repetition rate of 5 Hz (Eggins *et al.*, 1998), coupled to an Agilent HP7500 quadrupole ICP-MS system. Laser sampling was performed in an Ar atmosphere with He–H_2 (ratio 15:1) as a carrier gas with various beam diameters (30–250 μm) on several grains to evaluate cryptic zoning through samples if present. ^{29}Si (silicates) and ^{27}Al (spinels) were used as internal standard isotopes based on SiO_2 and Al_2O_3 concentrations measured by electron microprobe. NIST SRM 612 glass was used as an external standard and reference values were taken from Pearce *et al.* (1997) and Keller *et al.* (2008). BCR-2G glass was used as a secondary standard and reproducibility was generally better than 7%.

MINERAL CHEMISTRY

Olivine

Olivine is the most common mineral in the ultramafic terrane. With the exception of some pyroxenite dykes and late felsic inclusions, grains of olivine can be found in all stratigraphic levels of the ophiolite. In harzburgites, the chemical composition of olivine varies systematically with the stratigraphy on a scale of kilometres, but with local variations related to the presence of discordant rocks. An approximate stratigraphic sequence of the Massif du Sud has been established from the structural studies of Prinzhofer *et al.* (1980) and other geological mapping of the area. There is a trend for the average forsterite content $[Mg\# = Mg/(Mg + Fe^{2+})]$ of olivine in harzburgite to increase from 0·895 to 0·927 (Fig. 2b) with stratigraphic height: the lowest values ($Fo_{89–91}$) are found on the south-eastern coast (Yaté). In the vicinity of crustal zones, the Mg# of olivine in peridotite increases from 0·915 to 0·93 and then reaches a plateau at a value of $0·925 \pm 0·005$ in the lower dunite zone. In the transition zone and upper dunite zone, olivine is $\sim Fo_{90}$, which is clearly distinct from olivine in the lower dunite with Fo_{93}. The forsterite content of olivine drops in mafic cumulates to Fo_{84} in gabbros (Table 2).

NiO and MnO contents show small differences between lithologies. In harzburgites, no particular change in composition is seen with stratigraphy ($0·41 \pm 0·03$ wt % NiO; $0·12 \pm 0·02$ wt % MnO). Dunite olivines have a slightly lower NiO content than harzburgite but their MnO is the same. In the cumulate series, NiO content drops from upper mantle values (~0·37 wt %) to low values in gabbros (0·15 wt %). MnO has the opposite trend and increases from 0·12 to 0·25 wt % above the crust–mantle transition (Fig. 7; Table 2).

Olivine in harzburgite shows increasing contents of Al (4–175 ppm), Cr (5–238 ppm) and V (0·3–7·6 ppm), which correlate strongly with stratigraphy. Values increase 10–50 times between the lower peridotites and harzburgites of the higher part of the mantle section. In the uppermost zone, the presence of dunite and pyroxenite veins has a considerable influence on the trace element concentration in the surrounding harzburgite. Other trace elements that are measurable in olivine, such as Y, Ca and Ti, do not show any detectable variation within harzburgites.

Olivine in dunites follows the same trend with stratigraphy as present in harzburgite, with enrichment in Al (46–200 ppm), Cr (56–263 ppm) and V (2·8–8·3 ppm) up section. Higher calcium contents are also observed in dunites. This is probably related to the lack of pyroxenes

Table 2: Representative major and trace element compositions of olivine

Sample:	YA5	PRB34	PRB58b	PRB61f	PRB72b	PRB75	MDS34	MDS37	MDS43	MDS49
Lithology:	Harzburgite	Dunite	Harzburgite	Harzburgite	Dunite	Harzburgite	Dunite	Gabbro	Wehrlite	Dunite
Type:	tectonite	replacive	tectonite	tectonite	replacive	tectonite	cumulate	cumulate	cumulate	cumulate
n:	9	8	8	8	10	14	8	9	11	7
SiO_2	41·44 (27)	40·76 (66)	42·99 (54)	40·83 (39)	39·93 (40)	41·00 (69)	41·10 (35)	39·48 (26)	40·32 (41)	40·49 (37)
TiO_2	n.a.	b.d.l.	b.d.l.	b.d.l.	b.d.l.	b.d.l.	b.d.l.	b.d.l.	b.d.l.	b.d.l.
FeO	8·97 (8)	8·04 (7)	8·22 (12)	7·84 (22)	7·69 (9)	7·80 (33)	10·83 (12)	11·90 (14)	10·04 (14)	9·44 (13)
MnO	0·13 (2)	0·13 (1)	0·11 (1)	0·11 (1)	0·12 (2)	0·11 (2)	0·15 (2)	0·19 (1)	0·16 (1)	0·16 (1)
NiO	0·42 (1)	0·37 (1)	0·37 (3)	0·49 (10)	0·40 (2)	0·48 (16)	0·29 (1)	0·31 (2)	0·33 (1)	0·32 (2)
CoO	n.a.	0·02 (2)	b.d.l.	0·02 (2)	0·02 (1)	0·03 (2)	0·02 (1)	0·03 (1)	0·02 (1)	b.d.l.
MgO	49·80 (22)	51·64 (67)	50·61 (60)	52·19 (34)	51·45 (23)	51·90 (82)	49·43 (37)	47·97 (23)	48·93 (27)	49·76 (34)
CaO	0·03 (1)	0·10 (2)	b.d.l.	0·02 (1)	b.d.l.	0·03 (2)	0·04 (1)	0·04 (1)	0·20 (3)	0·04 (1)
Sum	100·89 (34)	102·09 (64)	102·43 (117)	101·57 (63)	99·74 (56)	101·43 (124)	101·89 (79)	99·97 (35)	100·05 (57)	100·26 (60)
Si	1·00 (0)	0·98 (0)	1·02 (0)	0·98 (0)	0·98 (0)	0·99 (1)	0·99 (0)	0·98 (0)	0·99 (0)	0·99 (0)
Ti	n.a.	b.d.l.	b.d.l.	b.d.l.	b.d.l.	b.d.l.	b.d.l.	b.d.l.	b.d.l.	b.d.l.
Fe	0·18 (0)	0·16 (0)	0·16 (0)	0·16 (0)	0·16 (0)	0·16 (1)	0·22 (0)	0·25 (0)	0·21 (0)	0·19 (0)
Mn		tr.	tr.	tr.	tr.	tr.	tr.	tr.	tr.	tr.
Ni	0·01 (0)	0·01 (0)	0·01 (0)	0·01 (0)	0·01 (0)	0·01 (0)	0·01 (0)	0·01 (0)	0·01 (0)	0·01 (0)
Co	n.a.	tr.	b.d.l.	tr.	tr.	tr.	tr.	tr.	tr.	b.d.l.
Mg	1·80 (1)	1·86 (1)	1·79 (1)	1·87 (1)	1·88 (1)	1·86 (1)	1·78 (0)	1·78 (1)	1·79 (1)	1·81 (1)
Ca	tr.	tr.	b.d.l.	tr.	b.d.l.	tr.	tr.	tr.	0·01 (0)	tr.
Σcat	3·00 (0)	3·02 (0)	2·98 (0)	3·02 (0)	3·02 (0)	3·01 (1)	3·01 (0)	3·02 (0)	3·01 (0)	3·01 (0)
Mg#	0·908 (0)	0·920 (0)	0·916 (2)	0·922 (0)	0·923 (1)	0·922 (0)	0·891 (1)	0·878 (0)	0·897 (0)	0·904 (0)
n	5	8	8	7	7	5	8	8	8	7
Li	1·4 ± 0·2	1·0 ± 0·2	0·3 ± 0·1	0·6 ± 0·1	1·1 ± 0·1	0·4 ± 0·1	1·4 ± 0·4	0·4 ± 0·0	1·1 ± 0·1	1·3 ± 0·5
Al	43 ± 61	94 ± 44	179 ± 69	122 ± 25	157 ± 28	109 ± 29	93 ± 12	110 ± 127	97 ± 96	123 ± 149
P	75 ± 9	6·6 ± 0·2	6·3 ± 0·6	4·0 ± 0·3	6·5 ± 0·3	4·5 ± 0·3	38·5 ± 5·7	9·2 ± 0·9	27·1 ± 1·6	8·3 ± 0·9
Ca	305 ± 72	843 ± 114	440 ± 47	310 ± 79	600 ± 97	332 ± 49	518 ± 92	288 ± 180	1838 ± 177	525 ± 287
Sc	4·9 ± 0·1	5·0 ± 0·6	4·0 ± 0·4	4·1 ± 0·3	4·6 ± 0·5	4·3 ± 0·4	6·1 ± 0·6	3·8 ± 0·4	5·9 ± 2·0	5·0 ± 0·6
V	0·9 ± 0·2	5·4 ± 2·1	7·3 ± 0·6	3·9 ± 0·6	4·5 ± 0·7	3·1 ± 0·5	1·7 ± 0·2	1·8 ± 0·4	1·5 ± 0·4	1·2 ± 0·3
Ti	4·7 ± 1·1	5·7 ± 1·9	2·5 ± 0·8	0·5 ± 0·0	3·0 ± 0·4	0·6 ± 0·1	7·4 ± 1·3	5·5 ± 1·1	6·8 ± 5·3	5·1 ± 1·1
Cr	266	133 ± 63	225 ± 18	136 ± 52	190 ± 36	162 ± 40	58 ± 33	35 ± 12	73 ± 15	69 ± 39
Mn	n.a.	1377 ± 24	1397 ± 16	1307 ± 24	1280 ± 17	1344 ± 16	1568 ± 17	2175 ± 18	1479 ± 13	1818 ± 16
Co	139 ± 7	140 ± 3	148 ± 1	135 ± 2	136 ± 2	139 ± 1	127 ± 1	198 ± 3	143 ± 2	148 ± 2
Ni	3048 ± 138	3106 ± 234	3411 ± 53	2919 ± 116	3018 ± 39	3011 ± 56	2307 ± 25	2627 ± 72	2555 ± 16	2597 ± 48
Zn	n.a.	48 ± 5	63 ± 1	43 ± 2	54 ± 1	47 ± 1	36 ± 2	136 ± 163	40 ± 3	42 ± 1

n.a., not analysed; b.d.l., below detection limit; tr., trace; numbers in parentheses are standard deviation applied to the last digit.

available for subsolidus re-equilibration, keeping Ca values in olivine closer to the primary magmatic concentrations. A distinctive enrichment in Al, Cr, V and Ti is also observed in the olivine of dunite bodies compared with the residual harzburgite, whereas Ni, Co and Li are lower. In the transition zone and gabbro units, cumulus olivine has lower Ni, Cr, and V, and is enriched in Y, Mn and P in comparison with residual peridotites. The concentration of some trace elements (Cr, Mn, Co) is highly dependent on modal composition and notably the amount of pyroxene and oxides in the crustal cumulates, and varies between gabbro and surrounding ultramafic cumulates (Table 2).

Orthopyroxene

The chemical composition of orthopyroxene in the harzburgite mirrors the behaviour of olivine. Mg# increases from 0·899 to 0·932 from the east coast (lower levels) to

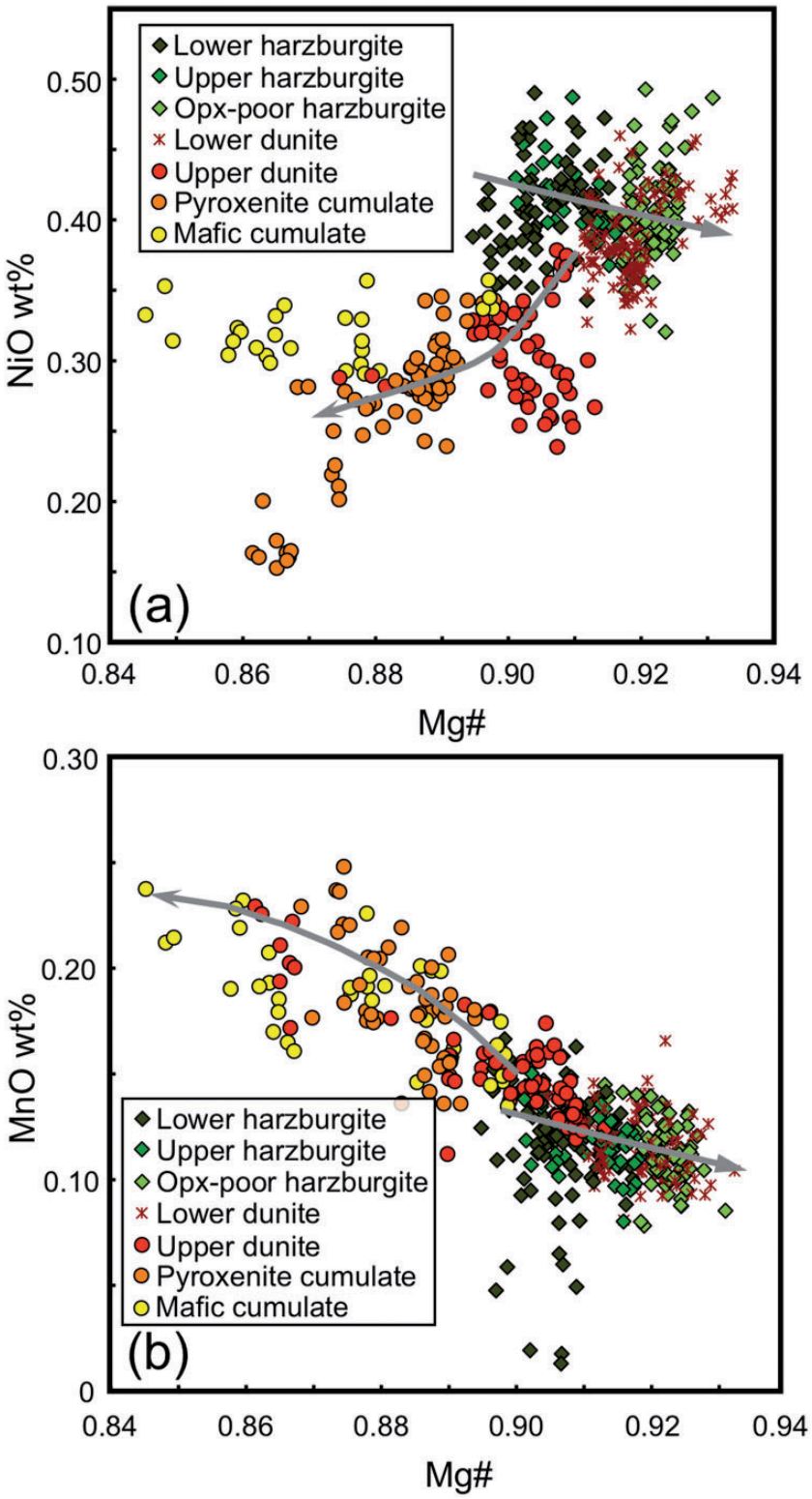

Fig. 7. Major element data for olivine. (a) Harzburgites increase in Mg# and NiO within the stratigraphy. The field for lower dunites overlaps with the upper harzburgite field with slightly lower NiO contents owing to replacive reaction (Kubo, 2002). Olivine from crustal cumulates displays a drop in NiO content and Mg# along with the evolution of the cumulates. (b) Olivine shows the opposite trend with decreasing MnO with increasing Mg# from deep to shallow mantle levels and increasing MnO content from upper cumulate dunite to gabbros. Arrows show an increasing depletion trend in mantle (increasing Mg#) and fractional crystallization (decreasing Mg#).

the dunite zone. Calcium shows a weak positive correlation with Mg# and varies from ~0·35 to 1·05 wt % CaO. Al_2O_3 and more particularly Cr_2O_3 are highly correlated with Mg#. Alumina varies from ~0·65 to ~1·5 wt % and Cr_2O_3 from 0·20 to 0·85 wt % from the lower to the uppermost harzburgite and the lower dunite zone. The corresponding Cr# [Cr/(Cr + Al)] increases from 0·20 in the lower to 0·27 in the upper harzburgite, in agreement with an increasing degree of depletion (Fig. 8) whereas Al_2O_3 contents are likely to be the result of subsolidus re-equilibration with olivine. In the mafic cumulates, orthopyroxenes are higher in alumina (2 ± 0·5 wt %) and show strong variation in CaO content from 0·5 to 3 wt %. Cr_2O_3 decreases from 0·8 wt % in the ultramafic cumulates to 0·5 wt % in gabbronorites and the Cr# decreases from 0·2 to 0·09 (Fig. 8; Table 3).

Trace elements in orthopyroxene porphyroclasts in the harzburgite also display systematic behaviour. Titanium and zirconium contents decrease by a factor of 100 between the eastern harzburgite and olivine-rich harzburgite in the uppermost mantle (Fig. 9). However, upper harzburgites that were collected in the vicinity of major melt pathways (dykes and channels) seem to have experienced a later episode of metasomatic enrichment in elements such as Zr and V, and can show intermediate concentrations between harzburgite and gabbros (Table 4). Additionally, variations of some trace elements [large ion lithophile elements (LILE), Pb, Sr] within a single hand specimen can be due to local conditions such as serpentinization reactions.

Orthopyroxenes in cumulates have high contents of titanium, vanadium and heavy rare earth elements (HREE), but other trace element contents are similar to those for orthopyroxene from the residual peridotites. Chondrite-normalized REE abundances in orthopyroxene display smooth patterns, with a steep increase from light REE (LREE) to HREE. The overall pattern in the mafic rock is similar to that of the harzburgites, although the absolute concentration of HREE is significantly higher in the mafic rocks (Fig. 10). Some orthopyroxenes from the harzburgites display La enrichment, which could be related to localized reaction with a fluid phase.

Clinopyroxene

Primary clinopyroxene is absent from the peridotites of the Massif du Sud. As a consequence, clinopyroxene analyses obtained for these rocks are mostly from exsolution in orthopyroxene porphyroclasts or from spinel–pyroxene symplectites. The Mg-number is higher than for orthopyroxene (0·938–0·956), and Al_2O_3 and Cr_2O_3 have a behaviour analogous to that in the orthopyroxene host. Alumina is 1·0 ± 0·2 wt % and increases only slightly at higher stratigraphic levels, whereas Cr_2O_3 increases from 0·4 to 1·2 wt % up section. CaO shows an opposite trend with respect to orthopyroxene as a result of subsolidus re-equilibration (see Supplementary Data Electronic Appendix 1, available for downloading at http://www.petrology.oxfordjournals.org). Clinopyroxenes from the east coast have 26 wt % CaO, but only 22·5 wt % CaO in the olivine-rich harzburgite of the uppermost mantle. In the cumulate series, clinopyroxene is a primary and dominant phase with decreasing Mg# (0·947–0·871) and variable concentrations of Al_2O_3 (1·7–3·1 wt %). Cr_2O_3 is constant at 1·1 ± 0·3 wt % and CaO decreases steadily from 25 to 20 wt % with decreasing Mg-number.

The trace element patterns of clinopyroxenes from gabbros feature low LILE and LREE and enrichment towards HREE (Fig. 11; Table 5). There is a slight negative anomaly in Sr and Eu, and patterns are similar to those reported by Marchesi *et al.* (2009) from the same locality. No Sr and Eu anomalies have been observed in clinopyroxene from microgabbronorite dykes. In dunites and cpx–plag-impregnated dunites, moderate positive europium and strontium anomalies can be present.

Spinel

The chemical composition of spinels is difficult to characterize, as variation can occur from grain to grain within a single sample. A similar scatter of spinel compositions has been observed in several ophiolites; for example, the Bay of Islands, Oman and Mirdita ophiolites (Bédard & Hébert, 1998; Arai *et al.*, 2006; Morishita *et al.*, 2011). These variations are related to morphology (blebs, symplectite), serpentinization (magnetite and iron-rich spinels *sensu lato*) and minor variations within single grains. Nevertheless, some major trends are visible in larger spinel blebs. Spinels in the harzburgite are magnesiochromites with Mg# = 0·5 ± 0·1 wt % and a high Cr# [= Cr/(Cr + Al + Fe^{3+})] of 0·68 ± 0·02. TiO_2 contents are slightly higher in deep harzburgite spinels (>0·08 wt % TiO_2) than in olivine-rich harzburgite (<0·05 wt % TiO_2) whereas V shows a weak inverse trend from ~0·09 to 0·26 wt % V_2O_3 (see Supplementary Data Electronic Appendix 1).

The Mg# of chromite from the lower dunite zone is the same as in the harzburgite, but the Cr# is slightly higher (0·72 ± 0·02). The Cr# and Cr_2O_3 in spinel from the upper dunite zone are considerably below values found in the lower dunite zone. Spinel in the upper dunite zone has a relatively high Mg# (~0·6), but these values drop progressively towards the gabbroic rocks to ~0·4. Cr# is 0·55 ± 0·04 and decreases slightly from the transition zone to the gabbros (Fig. 12). V_2O_3 contents range broadly between 0·13 and 0·50 wt % with no systematic differences between dunite cumulates and pyroxene-bearing cumulates.

Plagioclase

In the main ophiolite sequence, plagioclase occurs only within clinopyroxene-bearing cumulates lying above the

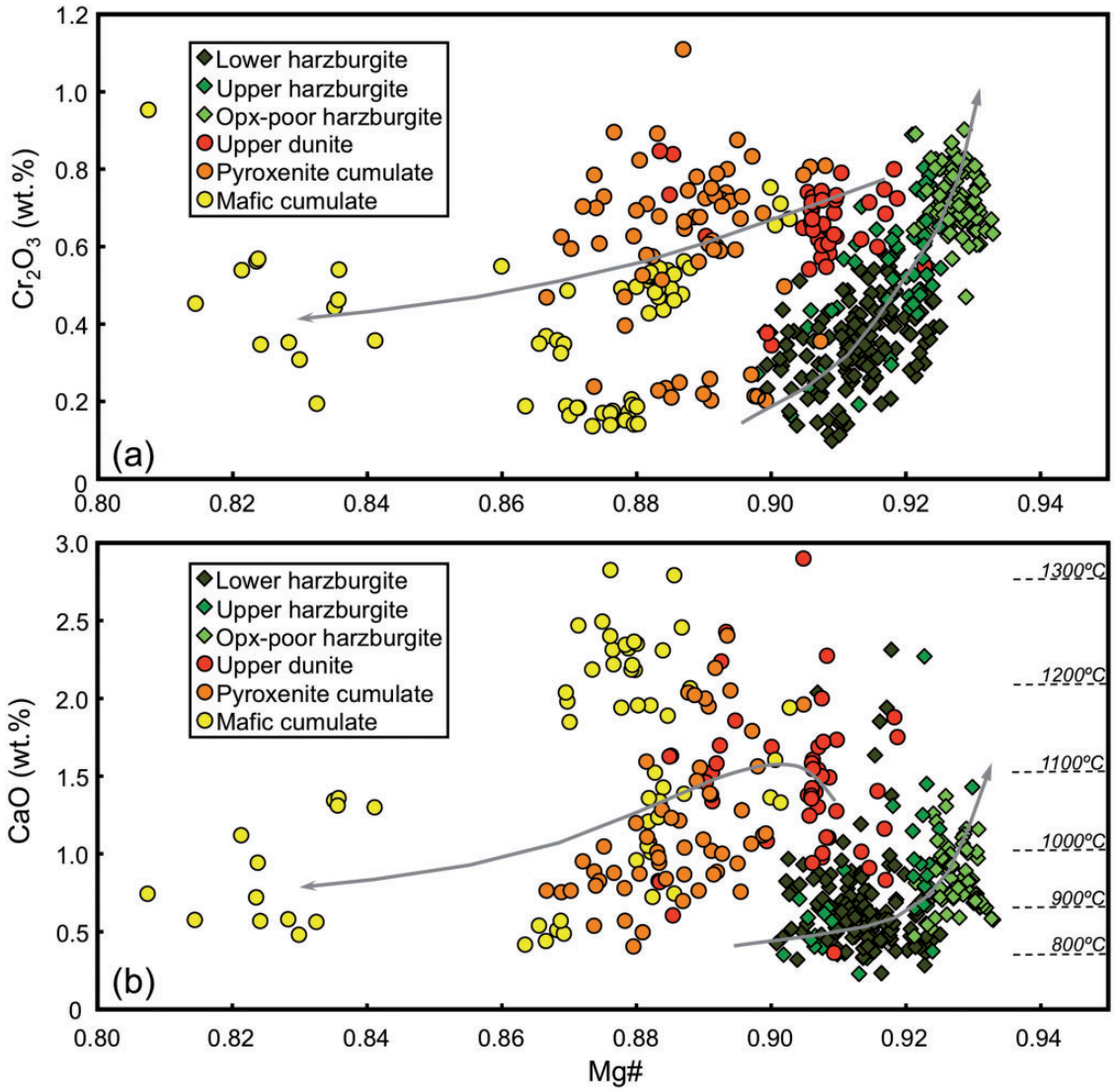

Fig. 8. Major element composition of orthopyroxene. (a) Mg# vs Cr_2O_3 (wt %) shows a strong increase in Cr_2O_3 upwards within the stratigraphy. Ultramafic cumulates (dunites, pyroxenites, wehrlites) have high Cr_2O_3 content but gabbronorites are mostly below 0·5 wt %. (b) Mg# vs CaO shows a very slight increase in CaO with stratigraphy in the harzburgite, strongly affected by subsolidus re-equilibration. Orthopyroxenes in cumulates are Ca-rich for ultramafic rocks such as dunites and pyroxenites. Dashed lines correspond to Ca-in orthopyroxene temperatures (solvus) coexisting with clinopyroxene in an Mg-rich system (Brey & Köhler, 1990). Arrows show an increasing depletion trend in mantle (increasing Mg#) and fractional crystallization (decreasing Mg#).

dunite zone in rocks that also contain clinopyroxene as an interstitial phase. The composition of the plagioclase is calcium-rich and ranges from An_{74}–An_{85} in some gabbro dikelets to $An_{87–92}$ in interstitial plagioclase of ultramafic cumulates and crustal gabbronorites. Little zoning has been observed in the plagioclase (see Supplementary Data Electronic Appendix 1).

Plagioclase in crustal cumulates have flat normalized REE patterns [$(La/Lu)_N = 0·40–1·08$] with high Eu, Sr and Be contents. Concentrations of V and Mn are also relatively high. Barium concentration is relatively low and Sr/Y is 1200 ± 400 (see Supplementary Data Electronic Appendix 1).

Other phases

Mafic and ultramafic rocks are considerably altered by hydrothermal and meteoric fluids, leading to the formation of abundant antigorite and lizardite. These two minerals are associated with magnetite and mainly replace olivine. High levels of Ni present in the peridotite also induce the formation of a twin nickelian serpentinization reaction whose products are commonly referred to as

Table 3: Representative major element compositions of orthopyroxene

Sample:	YR2	YA5	R34	PRB58b	PRB61f	PRB72b	PRB75
Lithology:	Harzburgite	Harzburgite	Harzburgite	Harzburgite	Harzburgite	Harzburgite	Harzburgite
Type:	tectonite	tectonite	tectonite	tectonite	tectonite	tectonite	tectonite
n:	4	18	7	22	20	6	10
SiO_2	57·49 (20)	57·84 (34)	58·60 (13)	59·61 (47)	59·43 (21)	58·40 (126)	58·87 (35)
TiO_2	0·01 (1)	0·02 (1)	b.d.l.	b.d.l.	b.d.l.	0·03 (2)	b.d.l.
Al_2O_3	1·10 (10)	0·97 (7)	1·53 (4)	1·48 (16)	1·34 (10)	1·31 (8)	1·23 (7)
Cr_2O_3	0·42 (11)	0·36 (4)	0·75 (4)	0·78 (10)	0·74 (7)	0·65 (5)	0·69 (6)
FeO	6·29 (10)	5·88 (8)	4·82 (3)	5·45 (26)	5·04 (10)	4·86 (4)	4·93 (5)
MnO	0·12 (7)	0·14 (1)	0·12 (2)	0·13 (2)	0·11 (1)	0·14 (0)	0·11 (2)
NiO	0·08 (0)	0·09 (2)	0·11 (1)	0·11 (4)	0·10 (2)	0·08 (1)	0·10 (2)
MgO	35·07 (8)	34·89 (26)	36·16 (21)	34·02 (68)	36·04 (28)	35·08 (29)	36·08 (16)
CaO	0·60 (12)	0·66 (20)	0·72 (3)	1·38 (40)	0·01 (1)	1·41 (5)	0·82 (4)
Na_2O	b.d.l.	b.d.l.	b.d.l.	b.d.l.	tr.	b.d.l.	b.d.l.
Sum	101·21 (15)	100·86 (53)	102·84 (28)	103·02 (65)	103·61 (35)	102·08 (150)	102·88 (43)
Si	1·96 (0)	1·98 (0)	1·96 (0)	1·99 (1)	1·98 (0)	1·97 (1)	1·97 (0)
Ti	tr.	tr.	b.d.l.	b.d.l.	b.d.l.	tr.	b.d.l.
Al	0·04 (0)	0·04 (0)	0·06 (0)	0·06 (1)	0·05 (0)	0·05 (0)	0·05 (0)
Cr	0·01 (0)	0·01 (0)	0·02 (0)	0·02 (0)	0·02 (0)	0·02 (0)	0·02 (0)
Fe	0·18 (0)	0·17 (0)	0·13 (0)	0·15 (1)	0·14 (0)	0·14 (0)	0·14 (0)
Mn	tr.	tr.	tr.	tr.	tr.	tr.	tr.
Ni	tr.	tr.	tr.	tr.	tr.	tr.	tr.
Mg	1·78 (0)	1·78 (1)	1·80 (1)	1·69 (3)	1·79 (1)	1·76 (2)	1·80 (1)
Ca	0·02 (0)	0·02 (1)	0·03 (0)	0·05 (1)	tr.	0·05 (0)	0·03 (0)
Na	b.d.l.	b.d.l.	b.d.l.	b.d.l.	tr.	b.d.l.	b.d.l.
Σcat	4·01 (0)	4·00 (0)	4·00 (0)	3·97 (1)	4·01 (0)	4·00 (1)	4·00 (0)
Mg#	0·91 (0)	0·91 (0)	0·93 (0)	0·92 (0)	0·93 (0)	0·93 (0)	0·93 (0)
Cr#	0·20 (3)	0·20 (1)	0·25 (1)	0·26 (2)	0·27 (2)	0·25 (1)	0·27 (3)

Sample:	MDS34	MDS36	MDS37	MDS39	MDS49	RP33	RP51
Lithology:	Dunite	Wehrlite	Gabbro	Wehrlite	Dunite	Websterite	Gabbro
Type:	cumulate	cumulate	cumulate	cumulate	cumulate	cumulate	cumulate
n:	11	4	19	8	11	12	11
SiO_2	56·69 (42)	60·01 (60)	57·60 (59)	56·33 (33)	56·25 (18)	56·29 (140)	57·89 (39)
TiO_2	0·04 (2)	0·03 (2)	0·03 (2)	0·04 (1)	0·03 (1)	0·02 (1)	0·03 (2)
Al_2O_3	1·75 (32)	2·07 (48)	1·64 (14)	1·90 (10)	1·85 (12)	2·85 (19)	1·50 (23)
Cr_2O_3	0·64 (10)	0·66 (20)	0·50 (4)	0·71 (6)	0·64 (6)	0·76 (15)	0·23 (2)
FeO	7·10 (29)	7·36 (30)	7·75 (21)	7·11 (17)	6·20 (10)	7·51 (35)	7·27 (36)
MnO	0·18 (3)	0·20 (3)	0·21 (2)	0·19 (2)	0·17 (2)	0·17 (1)	0·21 (2)
NiO	0·07 (2)	0·05 (3)	0·07 (2)	0·06 (1)	0·07 (1)	0·06 (1)	0·07 (1)
MgO	32·97 (30)	33·31 (48)	32·90 (53)	32·51 (24)	34·00 (31)	33·44 (75)	33·42 (69)
CaO	1·76 (53)	0·88 (19)	1·55 (82)	2·03 (24)	1·26 (27)	0·96 (22)	1·12 (31)
Na_2O	0·02 (1)	b.d.l.	0·01 (1)	0·03 (2)	0·01 (2)	0·01 (1)	b.d.l.
Sum	101·26 (32)	104·58 (66)	102·30 (66)	100·94 (66)	100·51 (38)	102·11 (199)	102·45 (33)

(continued)

Table 3: Continued

Sample:	MDS34	MDS36	MDS37	MDS39	MDS49	RP33	RP51
Lithology:	Dunite	Wehrlite	Gabbro	Wehrlite	Dunite	Websterite	Gabbro
Type:	cumulate	cumulate	cumulate	cumulate	cumulate	cumulate	cumulate
n:	11	4	19	8	11	12	11
Si	1·95 (1)	1·98 (1)	1·96 (1)	1·94 (0)	1·94 (0)	1·92 (1)	1·97 (0)
Ti	tr.	tr.	tr.	tr.	tr.	tr.	tr.
Al	0·07 (1)	0·08 (2)	0·07 (1)	0·08 (0)	0·08 (0)	0·11 (1)	0·06 (1)
Cr	0·02 (0)	0·02 (1)	0·01 (0)	0·02 (0)	0·02 (0)	0·02 (0)	0·01 (0)
Fe	0·20 (1)	0·20 (1)	0·22 (1)	0·21 (0)	0·18 (0)	0·21 (1)	0·21 (1)
Mn	0·01 (0)	0·01 (0)	0·01 (0)	0·01 (0)	0·01 (0)	tr.	0·01 (0)
Ni	tr.	tr.	tr.	tr.	tr.	tr.	tr.
Mg	1·69 (2)	1·64 (2)	1·67 (3)	1·67 (1)	1·75 (1)	1·70 (3)	1·70 (3)
Ca	0·06 (2)	0·03 (1)	0·06 (3)	0·07 (1)	0·05 (1)	0·04 (1)	0·04 (1)
Na	tr.	b.d.l.	tr.	tr.	tr.	tr.	b.d.l.
Σcat	4·01 (1)	3·97 (0)	4·00 (1)	4·01 (0)	4·01 (1)	4·01 (1)	3·99 (0)
Mg#	0·89 (0)	0·89 (1)	0·88 (0)	0·89 (0)	0·91 (0)	0·89 (1)	0·89 (1)
Cr#	0·20 (1)	0·18 (1)	0·17 (1)	0·20 (2)	0·19 (2)	0·15 (1)	0·09 (1)

'garnierite'. Talc and kaolinite are other alteration phyllosilicates likely to appear in plagioclase- or pyroxene-rich rocks. Sericite, hydrogrossular, prehnite and, more rarely, Ca-thompsonite also form after plagioclase.

Amphibole is generally a secondary hydrothermal mineral. However, rare minute inclusions of pargasite can be observed in some orthopyroxene porphyroclasts of some harzburgites.

Sulfides are frequent in the lower part of the ophiolite. Pentlandite is thought to be an early secondary phase and is rich in Ni (Ni/Fe = 1·2) and Co (2 wt % CoO). In most cases, Fe–Ni aggregates occur as a fine intergrowth of heazlewoodite and awaruite in olivine and serpentine. Graphite was also mentioned by Augé *et al.* (1999) in harzburgite, as well as a number of sulfides, oxides and alloys of platinoids associated with chromite and awaruite [see Augé & Legendre (1994), Augé & Maurizot (1995) and Augé *et al.* (1999) for details].

DISCUSSION

Stratigraphic sequence

Previous studies based on the geological mapping of the area (BRGM; Prinzhofer *et al.*, 1980; Augé & Maurizot, 1995) have given an overview of the stratigraphic sequence of the New Caledonia ultramafic rocks. The general aspect of the ophiolite is similar to that of other ultramafic–mafic sections studied in Oman, Cyprus, the Philippines, Newfoundland and Hokkaido (Violette, 1980; Girardeau & Nicolas, 1981; Pallister & Hopson, 1981; Smewing, 1981; Takashima *et al.*, 2002). It consists of an ultramafic root composed of harzburgite, a highly depleted zone of dunite in the upper part of the mantle section, and a transition zone with various ultramafic rocks and layered gabbros in the lower part of the oceanic crust (Fig. 3). Most of the upper part of the New Caledonia ophiolite has been tectonically detached or eroded, which leaves only a relatively small crustal section.

The geological maps of the BRGM are based on the major lithological differences between rock types. Some distinctions are based on field aspects, which do not reflect the official nomenclature of plutonic rocks (Streckeisen, 1976). Moreover, in this initial mapping, the harzburgite was presented as a homogeneous unit. Our petrographic observations coupled with geochemical data show that variations exist in single units that contain important information on the genesis and evolution of the New Caledonia ophiolite, one of the largest ultramafic massifs in the world.

The ultramafic sequence

The lithologies found in the Massif du Sud are extremely depleted in fertile components. No lherzolite has been reported in the ultramafic part and primary clinopyroxene is completely absent below the crust–mantle transition. Other harzburgitic ophiolites that show thicknesses similar to the Massif du Sud have lherzolite in the deepest part of their sections. Lherzolites in Oman (Takazawa *et al.*, 2003) and in the Balkans (Morishita *et al.*, 2011) have been interpreted either as peridotites that experienced a lower amount of partial melting or as zones with limited melt–mantle interaction (Godard *et al.*, 2000). In the Massif du Sud, no evident trends towards lherzolitic compositions

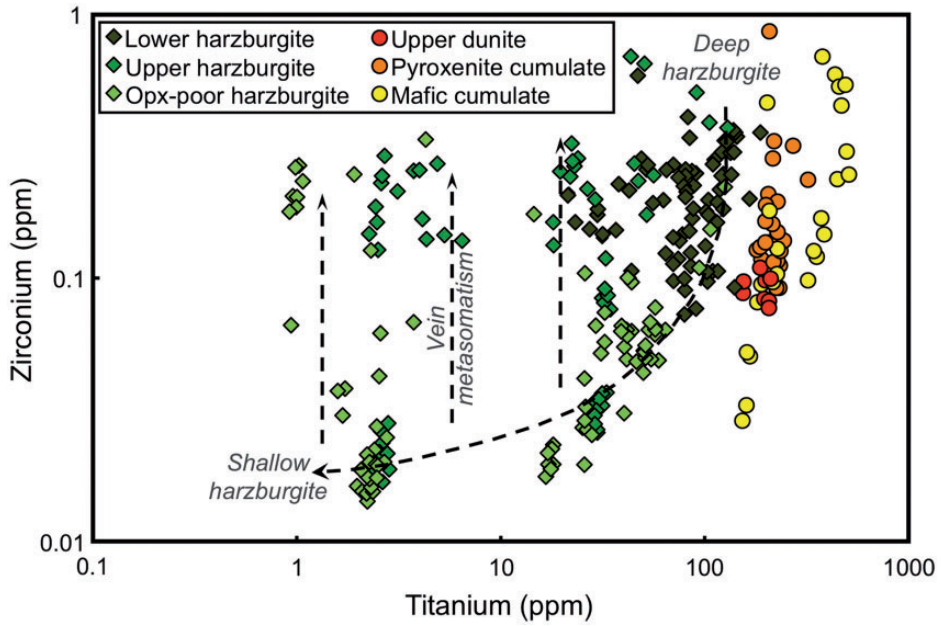

Fig. 9. The concentration of Zr and Ti in orthopyroxene decreases from the deepest harzburgite to the upper orthopyroxene-poor harzburgite. Samples outside the trend with higher zirconium contents are interpreted to represent cryptically metasomatized peridotites (McPherson *et al.*, 1996) near melt pathways.

are seen. The lherzolites in the northern massifs of Tiébaghi and Poum, which have sometimes been considered to represent the deeper part of the ultramafic nappe, include low-pressure plagioclase lherzolites and have recently been reinterpreted to be the result of refertilization of a depleted mantle section rather than lower amounts of partial melting (Ulrich *et al.*, 2010); as such these massifs would be a lateral variation of the Massif du Sud rather than a deeper level.

Our study of the harzburgites shows that there is a weak correlation between modal orthopyroxene with depth below the crust–mantle transition. At an outcrop scale, the lowest part of the mantle section shows an increase in chromite content in the harzburgite. Accessory phases such as sulfides and accompanying alloys are particularly abundant in the bottom 1000 m of the ultramafic terrane (Guillon & Lawrence, 1973) and have been described as locally reaching up to modal 10% in the lower harzburgite (Augé *et al.*, 1999). Other sulfide occurrences, notably at higher stratigraphic levels, are related to singularities in the mantle such as metasomatic events, veins and chromite pods.

The harzburgite has a tectonite fabric with metamorphic porphyroclastic textures (Mercier & Nicolas, 1975) (Fig. 4a). At depth, the peridotite is relatively homogeneous, but parallel alternation of harzburgite and dunite as a result of deformation with subsolidus recrystallization is observed in the higher zones (Nicolas, 1989) (Fig. 4b). These features are common in peridotites just below the crust–mantle transition and similar features have been extensively described in the Semail ophiolite (Boudier & Coleman, 1981; Lippard *et al.*, 1986). The high-temperature foliation and mineral lineation is mostly parallel to the crust–mantle boundary and extends 2000 m (Dupuy *et al.*, 1981) and 3500 m (Guillon, 1975) below the inferred base of the paleo-crust.

Although general petrological observations have been made on the peridotites of New Caledonia, there has hitherto been no correlation of the stratigraphy with geochemical data. The chemical composition of olivine and orthopyroxene in the harzburgite confirms the general stratigraphy with relatively steady variations from the eastern region towards the gabbroic units (Fig. 13). The main trends from bottom to top include an increase in Mg#, Cr#, V and Ca in olivine and orthopyroxene and a decrease in Ti and Zr in orthopyroxene and Li in olivine. Combined with the decreasing amount of modal orthopyroxene, these trends provide strong evidence for an increasing degree of partial melting in the mantle rocks, leaving residues with more refractory compositions.

The dunite complex

Since the early days when ophiolites were described as remnants of oceanic crust in New Caledonia and other localities (Auboin *et al.*, 1977), the nature of the dunite zone has remained enigmatic. These highly refractory rocks were interpreted as cumulates (Coleman, 1977; George, 1978; Pallister & Hopson, 1981; Elthon *et al.*, 1982; Smewing *et al.*, 1984; Lippard *et al.*, 1986; Coogan *et al.*, 2003; Clénet *et al.*, 2010) or as residues of extreme degrees

Table 4: Representative trace element compositions of orthopyroxene

Sample:	CY2	R34	PRB61f	PRB61e	PRB75	MDS32	MDS37	MDS49
Lithology:	Harzburgite	Harzburgite	Harzburgite	Harzburgite	Harzburgite	Gabbro	Gabbro	Dunite
Type:	tectonite	tectonite	tectonite	tectonite	tectonite	dyke	cumulate	cumulate
n:	8	7	12	4	13	6	8	2
Li	1·4 ± 0·2	1·6 ± 0·4	3·4 ± 0·7	2·3 ± 0·4	2·5 ± 1·5	0·5 ± 0·3	0·3 ± 0·2	1·8 ± 0·3
P	23·1 ± 0·9	22·2 ± 0·8	6·4 ± 0·5	18·4 ± 0·2	5·8 ± 0·5	33·8 ± 0·3	3·7 ± 0·7	5·6 ± 0·2
Sc	16·4 ± 0·9	15·8 ± 1·4	19·3 ± 1·1	19·4 ± 1·0	19·4 ± 1·1	39·2 ± 4·5	37·8 ± 1·5	36·6 ± 0·0
Ti	20 ± 9	3 ± 0	2 ± 0	30 ± 1	3 ± 0	355 ± 26	207 ± 9	155 ± 1
V	41 ± 2	39 ± 1	58 ± 2	75 ± 1	45 ± 2	133 ± 12	121 ± 3	74 ± 2
Cr	3804 ± 390	7544 ± 1762	4908 ± 356	4874 ± 172	5015 ± 161	2566 ± 1856	4450 ± 1216	4433 ± 25
Mn	964 ± 109	922 ± 25	1052 ± 43	1004 ± 25	1054 ± 30	1431 ± 209	1687 ± 16	1443 ± 31
Co	58·4 ± 0·9	59·3 ± 2·6	57·7 ± 3·0	57·7 ± 1·3	60·8 ± 1·0	64·5 ± 11·9	80·5 ± 0·8	55·8 ± 0·4
Ni	790 ± 24	834 ± 85	719 ± 60	731 ± 36	790 ± 36	677 ± 48	564 ± 4	556 ± 6
Cu	n.a.	0·82 ± 0·46	0·94 ± 0·46	0·07 ± 0·03	0·15 ± 0·22	0·39 ± 0·51	0·16 ± 0·15	0·30 ± 0·38
Zn	42 ± 1	42 ± 1	37 ± 2	43 ± 1	39 ± 1	56 ± 14	53 ± 1	32 ± 0
Sr	0·06 ± 0·03	0·03	0·02 ± 0·02	0·02 ± 0·01	0·03 ± 0·05	0·08 ± 0·08	0·08 ± 0·07	0·05 ± 0·01
Y	0·12 ± 0·01	0·01 ± 0·00	0·02 ± 0·00	0·09 ± 0·00	0·00 ± 0·00	1·15 ± 0·14	0·56 ± 0·04	0·52 ± 0·01
Zr	0·09 ± 0·02	0·02 ± 0·00	0·02 ± 0·00	0·03 ± 0·00	0·02 ± 0·01	0·13 ± 0·03	0·16 ± 0·13	0·09 ± 0·01
Nb	0·02 ± 0·00	0·02 ± 0·00	0·02 ± 0·00	0·03 ± 0·00	0·02 ± 0·00	0·11 ± 0·18	0·02 ± 0·01	0·02 ± 0·00
Cs	b.d.l.	b.d.l.	b.d.l.	b.d.l.	0·005 ± 0·002	0·11 ± 0·18	0·18	b.d.l.
Ba	b.d.l.	b.d.l.	0·01 ± 0·01	b.d.l.	0·02 ± 0·01	0·31 ± 0·43	0·004	b.d.l.
La	b.d.l.	0·03	b.d.l.	b.d.l.	0·002 ± 0·001	0·01 ± 0·00	0·01 ± 0·01	0·01 ± 0·00
Ce	b.d.l.	b.d.l.	b.d.l.	b.d.l.	0·005 ± 0·003	0·04 ± 0·04	0·01 ± 0·01	0·001
Pr	b.d.l.	b.d.l.	0·001	b.d.l.	0·001 ± 0·000	0·01 ± 0·01	0·001 ± 0·001	0·001
Nd	b.d.l.	b.d.l.	0·004	b.d.l.	b.d.l.	b.d.l.	0·01 ± 0·00	0·01
Sm	b.d.l.	b.d.l.	b.d.l.	b.d.l.	b.d.l.	0·02 ± 0·01	0·01 ± 0·00	b.d.l.
Eu	b.d.l.	0·01	0·001	b.d.l.	b.d.l.	0·01	0·004 ± 0·001	b.d.l.
Gd	b.d.l.	b.d.l.	0·004	b.d.l.	b.d.l.	0·04 ± 0·00	0·02 ± 0·00	b.d.l.
Tb	b.d.l.	b.d.l.	0·001	b.d.l.	b.d.l.	0·01 ± 0·00	0·01 ± 0·00	0·005
Dy	0·03 ± 0·01	b.d.l.	0·003 ± 0·000	0·02	0·003	0·13 ± 0·01	0·07 ± 0·01	0·05 ± 0·00
Ho	0·01 ± 0·00	b.d.l.	0·001 ± 0·000	0·01	b.d.l.	0·04 ± 0·01	0·02 ± 0·00	0·02 ± 0·00
Er	0·02 ± 0·00	b.d.l.	0·004 ± 0·001	b.d.l.	b.d.l.	0·18 ± 0·02	0·09 ± 0·01	0·09 ± 0·00
Tm	0·01 ± 0·00	b.d.l.	0·001 ± 0·000	b.d.l.	0·001 ± 0·000	0·03 ± 0·01	0·02 ± 0·00	0·02 ± 0·00
Yb	0·04 ± 0·01	b.d.l.	0·011 ± 0·002	0·03 ± 0·01	0·01 ± 0·00	0·30 ± 0·04	0·13 ± 0·01	0·18 ± 0·01
Lu	0·01	b.d.l.	0·003 ± 0·001	0·005 ± 0·000	0·002 ± 0·001	0·05 ± 0·01	0·02 ± 0·00	0·03 ± 0·00
Hf	b.d.l.	b.d.l.	b.d.l.	b.d.l.	0·002	0·01	0·01 ± 0·00	0·01
Ta	b.d.l.	b.d.l.	0·001	b.d.l.	b.d.l.	b.d.l.	0·002 ± 0·001	b.d.l.
Pb	b.d.l.	b.d.l.	0·004 ± 0·002	0·03 ± 0·01	0·01 ± 0·01	0·43 ± 0·78	0·04 ± 0·06	b.d.l.
Th	b.d.l.	b.d.l.	b.d.l.	b.d.l.	0·002	0·005		b.d.l.
U	b.d.l.	b.d.l.	0·002 ± 0·002		0·002 ± 0·001	b.d.l.	0·003 ± 0·002	b.d.l.

of partial melting (Sinton, 1977; Nicolas *et al.*, 1981; Nicolas & Prinzhofer, 1983; Benn *et al.*, 1988; Boudier & Nicolas, 1995; Jousselin & Nicolas, 2000; Yumul, 2004; Zhou *et al.*, 2005). Most geological mapping in ophiolites has neglected the variations that exist within the dunite zones. Instead, these units are often mapped as homogeneous bodies (Prinzhofer *et al.*, 1980) and it has, implicitly if not explicitly, been assumed that the entire dunite complex is the result of a single petrogenetic process.

The dunite zone in the Massif du Sud ophiolite is unusually well developed in comparison with other ophiolites, with a thickness of 600 ± 100 m (Prinzhofer *et al.*, 1980)

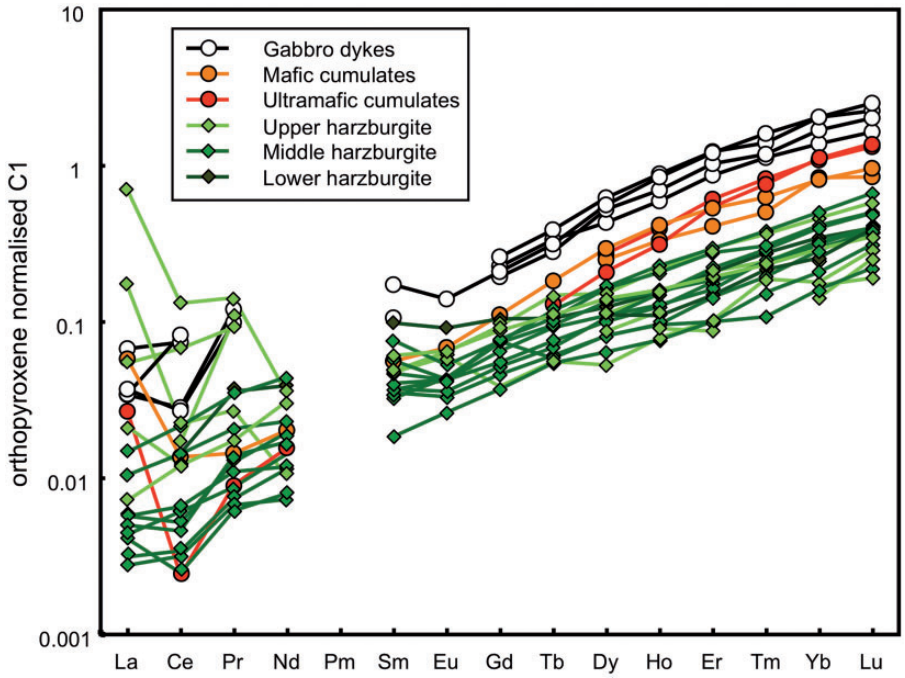

Fig. 10. Rare earth element patterns of orthopyroxene normalized to Cl chondrite (McDonough & Sun, 1995). Dark to light green line patterns are orthopyroxene porphyroclasts in harzburgite from deep to shallow position in the mantle section.

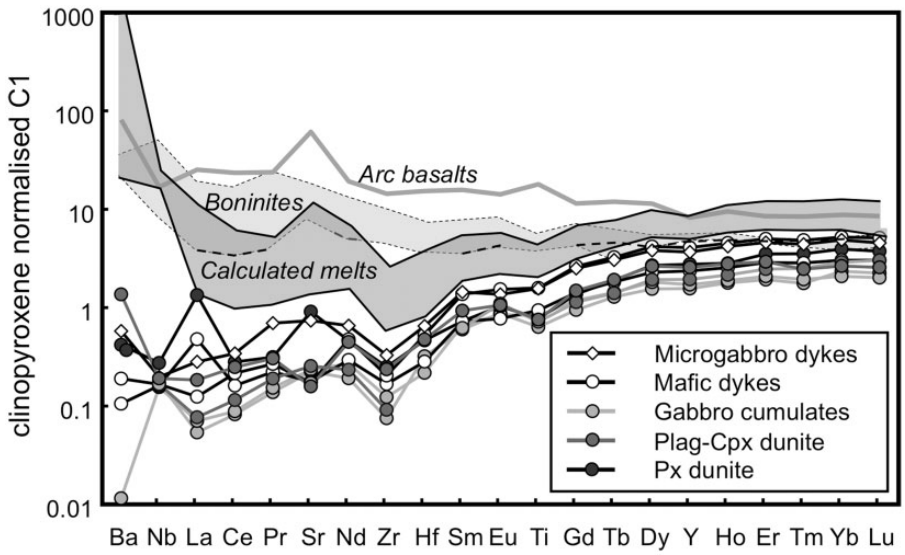

Fig. 11. Cl-normalized trace element patterns of clinopyroxene from transition zone rocks. Filled symbols are crustal cumulates and white symbols are mafic dykes. The dark grey shaded zone is the field of calculated melts for the mafic dykes using the partition coefficients for cpx–melt from Hauri *et al.* (1994) and Zack *et al.* (1997). The light grey shaded area is a compilation of boninite compositions (Sobolev & Danyushevsky, 1994; Kelemen *et al.*, 2003; Garrido *et al.*, 2007). The bold dashed line indicates the calculated REE contents of boninite melts from Kohistan clinopyroxenes (Garrido *et al.*, 2007). The grey line is the average composition of arc basalts from the Aleutian arc (Kelemen *et al.*, 2003).

(Fig. 3). A cumulate origin has been proposed based on grain morphologies and its layered fabric (Cassard *et al.*, 1981; Dupuy *et al.*, 1981; Nicolas & Prinzhofer, 1983; Augé *et al.*, 1999; Cluzel *et al.*, 2001; Picard *et al.*, 2004). Conversely, the compositions of the rocks and impregnation textures have been used to support a replacive origin of the dunite zone (Nicolas & Prinzhofer, 1983; Marchesi *et al.*, 2009).

Table 5: Trace element compositions of clinopyroxene

Sample:	MDS32	MDS37	MDS49	PRB49b	PRB49a
Lithology:	Gabbro	Gabbro	Dunite	Gabbro	Microgabbro
Type:	dyke	cumulate	cumulate	dyke	dyke
n:	10	8	4	16	14
Li	2·1 ± 0·5	0·9 ± 0·2	4·3 ± 0·8	2·8 ± 3·1	2·3 ± 0·9
Be	b.d.l.	0·002	0·009 ± 0·007	0·006	0·019
P	30·3 ± 0·7	4·2 ± 1·2	10·3 ± 6·7	6·6 ± 6·3	55·8 ± 38·8
Sc	75 ± 4	71 ± 2	82 ± 8	65 ± 4	73 ± 10
Ti	697 ± 127	364 ± 33	340 ± 26	413 ± 31	686 ± 252
V	273 ± 19	242 ± 7	171 ± 15	440 ± 50	461 ± 68
Cr	6288 ± 3555	7325 ± 1377	9424 ± 461	6929 ± 355	5800 ± 1596
Mn	973 ± 118	1220 ± 39	1167 ± 283	1125 ± 51	1144 ± 98
Co	31 ± 5	42 ± 2	27 ± 3	42 ± 2	46 ± 5
Ni	403 ± 24	351 ± 12	313 ± 25	453 ± 41	428 ± 81
Cu	0·33 ± 0·30	17·0 ± 47·1	2·30 ± 1·75	1·22 ± 2·12	9·5 ± 13·4
Zn	20·1 ± 4·3	21·3 ± 1·5	11·0 ± 3·1	28·3 ± 2·9	42·1 ± 8·8
Rb	b.d.l.	0·01 ± 0·01	0·19 ± 0·28	0·04 ± 0·04	b.d.l.
Sr	1·2 ± 0·5	1·7 ± 0·2	6·6 ± 4·1	1·3 ± 0·9	5·3 ± 4·5
Y	6·4 ± 0·7	2·7 ± 0·2	4·3 ± 0·8	3·7 ± 0·4	5·8 ± 2·1
Zr	0·78 ± 0·22	0·47 ± 0·07	0·96 ± 0·38	0·64 ± 0·42	1·26 ± 0·73
Nb	0·04 ± 0·02	0·04 ± 0·00	0·07 ± 0·03	0·04 ± 0·01	0·05 ± 0·02
Cs	0·04 ± 0·02	b.d.l.	0·05	0·01 ± 0·01	0·05 ± 0·02
Ba	0·46 ± 0·33	0·03 ± 0·04	1·01 ± 1·22	0·25 ± 0·31	1·39 ± 1·25
La	0·03 ± 0·04	0·02 ± 0·00	0·32 ± 0·30	0·11 ± 0·10	0·07 ± 0·09
Ce	0·13 ± 0·12	0·05 ± 0·01	0·17 ± 0·03	0·10 ± 0·02	0·21 ± 0·13
Pr	0·02 ± 0·01	0·01 ± 0·00	0·03 ± 0·00	0·02 ± 0·01	0·06 ± 0·09
Nd	0·22 ± 0·07	0·12 ± 0·01	0·21 ± 0·06	0·13 ± 0·07	0·30 ± 0·15
Sm	0·20 ± 0·05	0·10 ± 0·01	0·11 ± 0·01	0·11 ± 0·03	0·21 ± 0·11
Eu	0·09 ± 0·01	0·05 ± 0·00	0·06 ± 0·00	0·04 ± 0·01	0·08 ± 0·05
Gd	0·52 ± 0·10	0·24 ± 0·02	0·27 ± 0·01	0·28 ± 0·05	0·50 ± 0·22
Tb	0·12 ± 0·02	0·05 ± 0·00	0·07 ± 0·01	0·07 ± 0·01	0·11 ± 0·05
Dy	1·03 ± 0·13	0·45 ± 0·03	0·66 ± 0·11	0·56 ± 0·08	0·94 ± 0·37
Ho	0·25 ± 0·03	0·10 ± 0·01	0·15 ± 0·02	0·14 ± 0·02	0·23 ± 0·09
Er	0·80 ± 0·08	0·33 ± 0·02	0·56 ± 0·09	0·46 ± 0·06	0·74 ± 0·25
Tm	0·12 ± 0·01	0·05 ± 0·00	0·09 ± 0·02	0·07 ± 0·01	0·11 ± 0·03
Yb	0·84 ± 0·07	0·34 ± 0·02	0·63 ± 0·11	0·49 ± 0·04	0·78 ± 0·22
Lu	0·13 ± 0·01	0·05 ± 0·00	0·09 ± 0·01	0·07 ± 0·01	0·11 ± 0·03
Hf	0·05 ± 0·02	0·02 ± 0·00	0·05 ± 0·02	0·03 ± 0·01	0·07 ± 0·04
Ta	0·05	b.d.l.	b.d.l.	b.d.l.	0·05 ± 0·04
Pb	0·09 ± 0·06	0·02 ± 0·03	0·79 ± 0·68	0·09 ± 0·12	1·88 ± 2·29
Th	b.d.l.	0·002 ± 0·001	0·01 ± 0·01	0·002 ± 0·002	0·04 ± 0·01
U	0·02	b.d.l.	0·04 ± 0·02	0·004 ± 0·003	0·05 ± 0·03

The transition from harzburgite to dunite occurs progressively over a section representing about 300 m, with an increasing amount of dunite pods within the upper harzburgite (Fig. 4d). Vermicular spinel overgrowths on pre-existing grains (Fig. 5) are very similar to the discordant dunites in the harzburgite sections, which are less controversially ascribed to the percolation of orthopyroxene-undersaturated melts (Kelemen et al., 1990) (Fig. 4c),

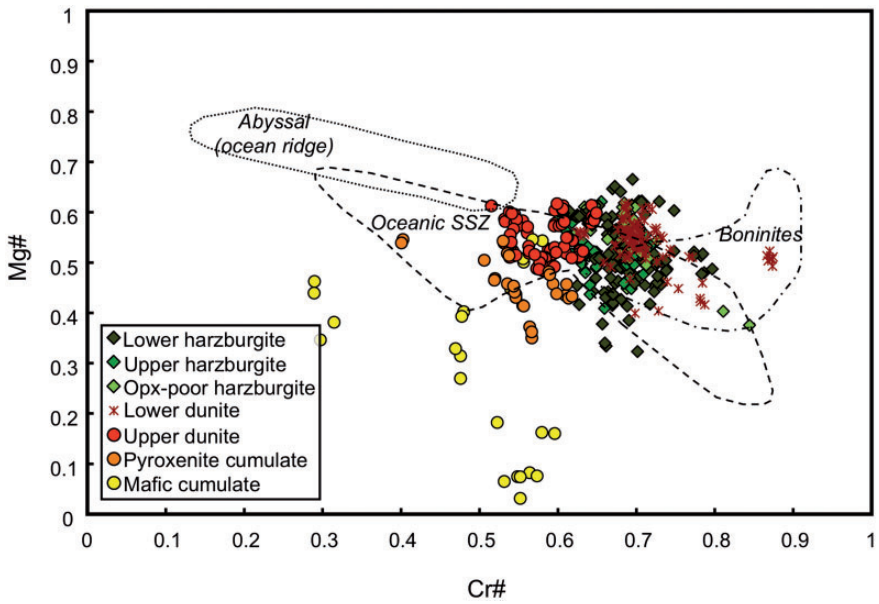

Fig. 12. The Mg# vs Cr# of spinels from the various rock types of the Massif du Sud. Harzburgites mainly lie in the fore-arc–oceanic SSZ field and are distinct from the abyssal peridotite field (Dick & Bullen, 1984). The boninite field (Metcalf & Shervais, 2008) includes a few peridotites. Spinels in replacive lower dunite and cumulus upper dunite have clearly different Cr#.

suggesting that these dunites were also formed by melt–peridotite interaction, consuming pyroxenes and precipitating olivine. The boundary is mapped where dunite lithologies become dominant over harzburgite. It is a very diffuse transition, which has also been observed in several other ophiolites; for example, Oman, Coto (Philippines) and Bay of Islands (Newfoundland) (Girardeau & Nicolas, 1981; Nicolas & Prinzhofer, 1983). The texture of the lower dunite zone is not fundamentally different from that of harzburgite and would be best described as porphyroclastic with syntectonic recrystallization leading to equigranular textures (Mercier & Nicolas, 1975). Plastic strain is strong in the lowest dunite and fades upward to disappear after a few hundred metres (Nicolas & Prinzhofer, 1983). In contrast, olivine crystals in the upper dunites are mainly polygonal and give an equigranular texture to the rock, characteristic of a cumulate.

The lower dunite zone is particularly homogeneous in terms of modal and chemical composition. The Mg# is as high as in the uppermost harzburgite and NiO contents are only slightly lower (Fig. 7). However, about 200 m within the dunite zone, the Mg# drops by 1–2% in olivine, and Ni, V and Cr tend to be lower, whereas MnO, Y_2O_3 and TiO_2 are higher (Figs 7 and 13). This difference is also reflected in spinel compositions, with Cr-number decreasing by 10% (Fig. 12), and a change in appearance from grains with vermicular overgrowths characteristic of the lower dunite, to rounded, sub-idiomorphic grains with frequent silicate inclusions in the upper dunite (Fig. 5).

The combination of these textural and geochemical features provides a solid discriminator for the origin of the massive dunites in the Massif du Sud. It shows that the transition between replacive (formed by interaction of melt with peridotite) and cumulus dunites (precipitating from melt without interactions with peridotite) occurs near the middle of the dunite zone. Therefore, the petrological transition between 'mantle' and 'crust' may occur within the dunite zone.

The crustal sequence

Four sections across the transition zone were mapped and sampled, providing a general comparison between areas close to each other (Fig. 3b). The crust–mantle transition evolves from simple dunite through impregnated dunite, to pyroxenite and then gabbro. The transition can be progressive over a few tens of metres or marked by sharp layers of different lithologies. Bulk-rock and mineral geochemistry for this ultramafic–mafic sequence has been reported by Marchesi *et al.* (2009). They interpreted this sequence as impregnation of replacive dunites by mafic melts. However, the micro-textures of cumulus dunite, as well as the major and trace element composition of olivine in dunite and wehrlite, in our studied sections are clearly different from the replacive dunite stratigraphically below, and olivine grains in the gabbros above. Moreover, the major and trace element compositions of pyroxenes and plagioclase that are poikilitic between olivine grains in ultramafic cumulates overlap with those found in the gabbros. Although our data are inconsistent with the model that the whole sequence originated from pervasive melt percolation in residual dunite, there is field evidence of interaction between gabbro sills and ultramafic

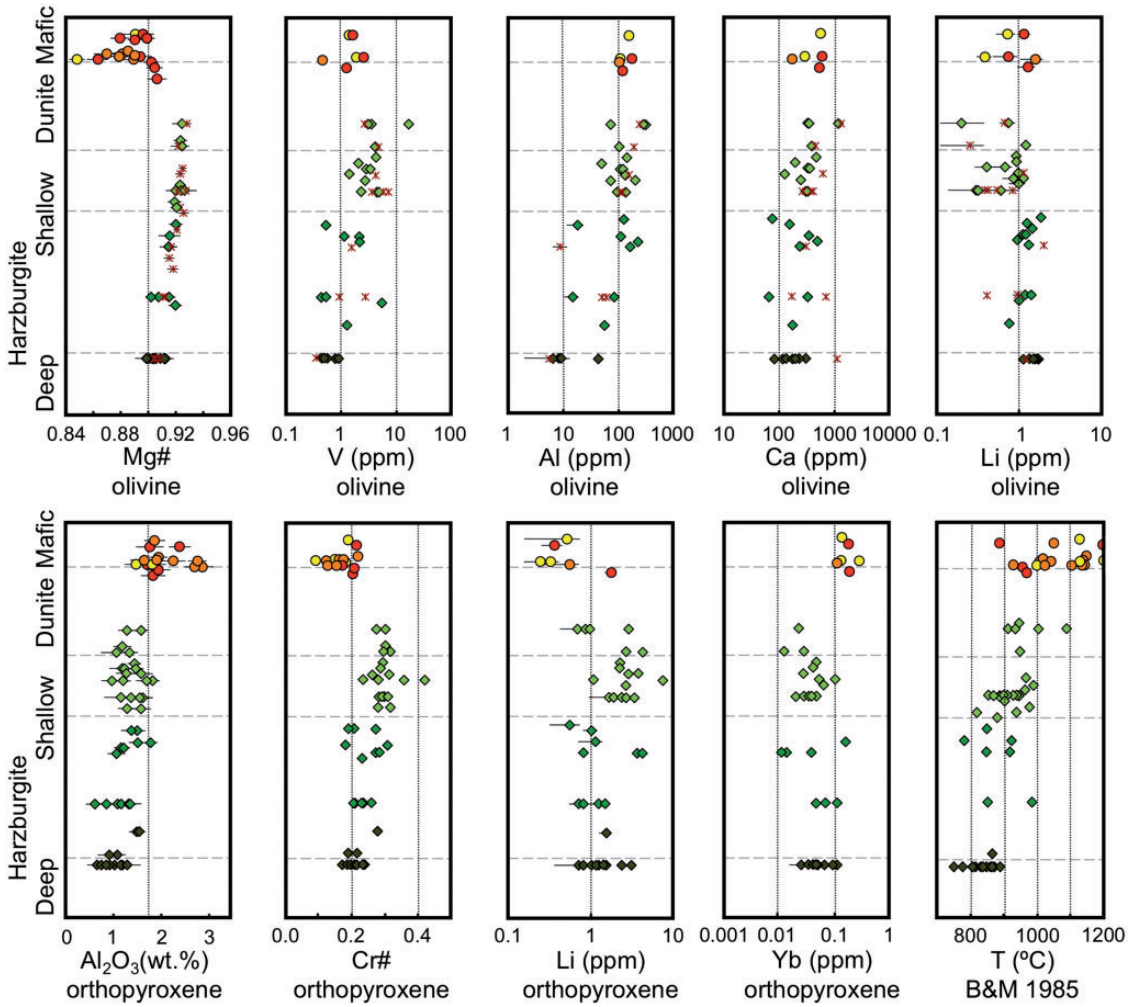

Fig. 13. Compositions of olivine and orthopyroxene for several major and trace elements and a temperature profile (Bertrand & Mercier, 1985) of the ophiolite for harzburgites (diamonds), replacive dunites (stars) and cumulate rocks (circles), which include dunite (red), pyroxenite (orange) and gabbro (yellow). Horizontal dashed lines represent limits between rock-types; vertical lines are for reference.

rocks at the local scale, such as selvages with decreasing modal content of plagioclase and clinopyroxene impregnation within the dunite (Fig. 6a–c). Structural observations and geochemistry suggest that the sources of melt impregnation in the dunite are the gabbro sills themselves. Such progressive and sequential mantle–crust sections (Fig. 3b) have been described in ophiolites of the Arabian peninsula (Benn *et al.*, 1988; Boudier & Nicolas, 1995) and, hence, could be a common phenomenon.

Clinopyroxene in gabbros and wehrlites is characterized by high Mg# of 0·90 and trace element patterns that display minimal Sr and Eu anomalies (Fig. 11), demonstrating that clinopyroxene crystallized from a primitive melt before plagioclase. This is not typical of the crystallization sequence in mid-ocean ridge basalts (MORB), but indicates lower alumina (as in ocean island basalts), or high H_2O (as in island arc basalts) or high pressure. The trace element pattern of this parental melt can be constrained using the partition coefficients for cpx–melt from Hauri *et al.* (1994) and Zack *et al.* (1997). The resulting melt composition is characterized by a small middle REE (MREE) depletion, small negative anomalies in Ti and Zr, a high Th/Nb ratio and very high Ba/Th ratio. These geochemical characteristics are very different from average MORB values (Jenner & O'Neill, 2012) and suggest an important shallow subduction contribution to the formation of these melts (Pearce *et al.*, 2005).

Magmatic and metamorphic conditions

Temperature

High-temperature fabrics are preserved in the peridotites. According to textural studies, the presence of a porphyroclastic assemblage (Mercier & Nicolas, 1975) would imply flow at relatively high temperature (1200–1350°C),

although some sub-types may reflect lower temperatures (~1100°C; Rampone *et al.*, 2010). The temperatures in the porphyroclastic spinel harzburgites were calculated using various techniques (Table 6). Calcium equilibrium between pyroxenes in the presence of olivine (Bertrand & Mercier, 1985; Brey & Köhler, 1990; Köhler & Brey, 1990) gives the most consistent results in their field of application, whereas geothermometers based on exchange of Mg and Fe^{2+} between olivine and spinel (Fabries, 1979; Roeder *et al.*, 1979; O'Neill & Wall, 1987) record subsolidus re-equilibration at temperatures below 700°C. The two-pyroxene thermometer is not applicable to the harzburgites because of the lack of primary clinopyroxene, although minimum temperatures can be obtained from the compositions of orthopyroxenes under the assumption that they represent equilibrium with clinopyroxene. This is reasonable as both cooling of an initially clinopyroxene-undersaturated orthopyroxene and subsolidus exchange of Ca with olivine will both tend to bring on saturation in clinopyroxene. Indeed, some clinopyroxene is evident as exsolution lamellae. Calculated two-pyroxene temperatures increase from the bottom peridotite (870–900°C) to the uppermost part of the ultramafic section (900–1000°C) (Fig. 13). This increase of temperature of the subsolidus equilibration is also documented in the increase of Al_2O_3 and Cr_2O_3 in orthopyroxene up section. The range of temperature shows that geochemical re-equilibration is present in all peridotites, with the lowest equilibration temperatures present in the deepest level of the Massif du Sud.

In the dunite zone, the absence of pyroxenes restricts the use of geothermometers. Olivine–spinel geothermometry gives subsolidus re-equilibration temperatures similar to the mantle. Ca-in-olivine temperatures are noticeably high in the dunite and reflect the lack of subsolidus equilibrium owing to the absence of pyroxene. Rare microscopic clinopyroxene grains are observed in dunite and could be interpreted as exsolution from olivine. In such cases, temperatures are between 1100 and 1280°C for dunite, 1050–1230°C for harzburgite and 1150–1350°C for the cumulates. These temperatures represent minimum values for the dunite as the magmatic assemblage olivine–clinopyroxene is absent in mantle rocks.

The cumulates offer more opportunities for geothermometry because the four-phase assemblage of olivine, orthopyroxene, clinopyroxene and plagioclase is present in a wide range of rocks. Textures show little evidence of subsolidus reactions. Application of pyroxene geothermometers (Bertrand & Mercier, 1985; Brey & Köhler, 1990) to gabbronorite sills gave 1100–1200°C, whereas ultramafic cumulates range from 950 to 1150°C (Fig. 13). These values overlap with the results of olivine–clinopyroxene thermometry, which give temperatures up to 1250°C.

Although the inverted geotherm seems counterintuitive, it is suggested that the cooling during obduction happened more slowly at the base of the ophiolite than in the crustal section. Slower cooling rates allowed longer re-equilibration times at lower temperatures and are in agreement with temperatures estimated for the metamorphic sole underlying the New Caledonia ophiolite (Cluzel *et al.*, 2012).

Pressure

In the lower part of the ophiolite, symplectites of chromite and pyroxenes are observed in the harzburgite (Fig. 5). Similar assemblages have been observed in other

Table 6: Average temperatures calculated using different geothermometers

Geothermometer		Lithology				
		Lower harzburgite	Upper harzburgite	Dunite	Ultramafic cumulates	Gabbronorite
Wells (1977)	(opx/cpx)	795 ± 106	983 ± 162		985 ± 109	1083 ± 69
Fabries (1979)	M^{2+}/M^{3+}(opx/ol/sp)	386 ± 83	416 ± 101		352 ± 106	382 ± 40
Roeder *et al.* (1979)	M^{2+}/M^{3+}(ol/sp)	640 ± 52	648 ± 108	634 ± 45	650 ± 39	696 ± 52
Bertrand & Mercier (1985)	Ca(opx/cpx)	831 ± 48	920 ± 52		1041 ± 92	1095 ± 61
Brey & Köhler (1990)	Ca(opx/cpx)	656 ± 164	876 ± 170		925 ± 138	1050 ± 81
Brey & Köhler (1990)	Ca(opx)	953 ± 76	973 ± 114		1057 ± 137	1079 ± 103
Köhler & Brey (1990)	Ca(ol/cpx)	1123 ± 50	1151 ± 67	1218 ± 88	1190 ± 57	1256 ± 90
Witt-Eickschen & O'Neill (2005)	Al/Cr(opx/sp)	1065 ± 88	1252 ± 77	1201 ± 48	1166 ± 84	1005 ± 119
Witt-Eickschen & O'Neill (2005)	Ni/Mg(ol/opx)	857 ± 38	902 ± 51	905 ± 98	896 ± 45	898 ± 78

peridotites such as Horoman or Tallante (Morishita *et al.*, 2003; Shimizu *et al.*, 2008; Rampone *et al.*, 2010) and are interpreted as the result of a garnet breakdown reaction Grt + Olv → Opx + Cpx + Sp (Field & Haggerty, 1994). The reconstructed compositions of these clusters are close to garnet stoichiometry, which supports this hypothesis. The high Cr content of the calculated garnet suggests homogenization of spinel compositions with the surrounding peridotite (Arai, 1994). In fact, a retrograde equilibration is consistent with estimated temperatures of ~850°C for the given assemblage. A pressure below 13 kbar is based on the absence of garnet in the peridotite (O'Neill, 1981) and mantle pyroxenite layers (Hirschmann & Stolper, 1996).

In the gabbros, the ol + opx + cpx + plag assemblage lacking garnet or spinel suggests pressures below 8 kbar (Müntener *et al.*, 2001; Garrido *et al.*, 2006). Alumina in pyroxene is highly dependent on pressure in plagioclase-rich rocks such as the New Caledonia gabbronorites and indicates pressures from 2 to 4 kbar for the mafic rocks of Montagne des Sources and Rivière des Pirogues (Herzberg, 1978; Gasparik, 1984; Borghini *et al.*, 2010). Such estimates are in agreement with geophysical studies in the South Loyalty Basin (Collot *et al.*, 1987), which is considered as the non-overthrust part of the New Caledonia ophiolite. The standard thickness of 6·5 km for the oceanic crust prior to obduction would provide ~2 kbar of pressure at the crust–mantle transition level.

Oxygen fugacity

Oxygen fugacity estimates can be made for the harzburgite and dunites as they contain orthopyroxene, olivine and spinel (O'Neill & Wall, 1987). Most ultramafic rocks lie in the range of FMQ − 1 to FMQ − 0 (where FMQ is the fayalite–magnetite–quartz buffer), which is in the field of sub-arc peridotites from Japan, New Ireland and Kamchatka (Arai & Ishimaru, 2008). Values obtained in the Massif du Sud for pristine peridotites are in the upper fO_2 range of abyssal peridotites (FMQ − 2·5 to FMQ − 0, Aldanmaz *et al.*, 2009) and are included in the field of mantle wedge environments (Brandon & Draper, 1996; Blatter & Carmichael, 1998; Parkinson & Arculus, 1999). Vanadium partitioning between olivine and orthopyroxene (Fig. 14) shows analogous behaviour to Cr and Al in the harzburgites. These parallel trends suggest that V is mainly present as V^{3+} in the harzburgites (Witt-Eickschen & O'Neill, 2005). However, the transition from the uppermost harzburgite to the oceanic crust is associated with a change in the partitioning of V compared with Cr and Al, which suggests that vanadium is increasingly in a V^{4+} state in the oceanic crust, becoming more concentrated in orthopyroxene, whereas aluminium does not show such behaviour (Mallmann & O'Neill, 2009).

Water

The crystallization sequence observed (olivine → pyroxene → plagioclase) in the crustal section in the Massif du Sud provides evidence for elevated water contents in the magmas. The early appearance of pyroxenes in cumulus dunite and the extensive delay in the saturation of plagioclase support a water-rich magmatic system (Feig *et al.*, 2006). The increase in Al in clinopyroxene with decreasing Mg# suggests that early cumulates crystallized under hydrous conditions with no saturation in plagioclase, following arc trends established in other ophiolites (Gaetani *et al.*, 1993; Jagoutz *et al.*, 2007; Koepke *et al.*, 2009) (Fig. 15). The high anorthite content of plagioclase also confirms this hypothesis as the liquidus of the Ab–An–H_2O system is considerably depressed near the calcium-rich end member. This allows the crystallization of high anorthite plagioclase at moderate temperatures.

The orthopyroxene content in the gabbros is also a specific feature, which suggests that the gabbronorites were formed from water-rich magmas at high oxygen fugacity (Grove & Baker, 1984). Relatively high water pressure is responsible for an increase in the primary phase volume of orthopyroxene and its crystallization at lower temperatures (Juster *et al.*, 1989). In other ophiolites, gabbronorites often contains magmatic amphibole, confirming the hydrous nature of the parental mafic magma (Boudier *et al.*, 2000). In the Massif du Sud, the absence of primary hydrous minerals is linked to the high crystallization temperature of the magmas. Geothermometry calculations indicate crystallization temperatures between 1100 and 1200°C for the gabbros, which are too high a temperature range for amphibole to be a liquidus phase (Holloway & Burnham, 1972).

Recent field observations on wehrlite pods in the Oman peridotite have shown that conditions near water-saturation are necessary to produce such rocks (Feig *et al.*, 2006; Koepke *et al.*, 2009). Experimental studies on hydrous primitive arc melts have shown that clinopyroxene is an early crystallizing phase (Müntener *et al.*, 2001). The clinopyroxene-bearing cumulates in the Massif du Sud share similarities with the lower part of the layered complex of Chilas in the Kohistan arc and the Tonsina sequence in the Talkeetna arc, Alaska, which are interpreted to have originated from hydrous melts (DeBari & Coleman, 1989; Jagoutz *et al.*, 2007).

Environment for the formation of the crust–mantle section

Spinel–pyroxene symplectites in the harzburgites are interpreted as a breakdown product of garnet, providing evidence for exhumation from pressures higher than 20 kbar to ~2–4 kbar at the time of gabbro emplacement. We expect the first stage of exhumation from garnet-peridotite to spinel-peridotite to be coincident with initial melting of

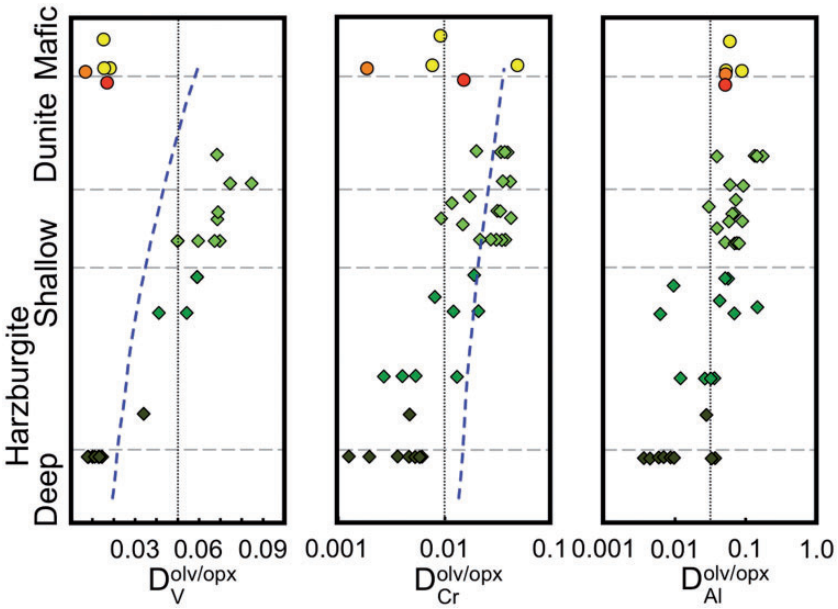

Fig. 14. Partition coefficient between olivine and orthopyroxene for V, Cr and Al as a function of stratigraphy for harzburgite (diamonds) and crustal cumulates (circles) including dunite (red), pyroxenite (orange) and gabbro (yellow). Although these elements show a similar trend in the mantle, partitioning behaviour diverges in the transition zone and the crust. Horizontal dashed lines represent limits between rock-types; vertical lines are for reference. The dashed blue curves are partition coefficients for V and Cr from Witt-Eickschen & O'Neill (2005) based on the calculated temperatures (Bertrand & Mercier, 1985).

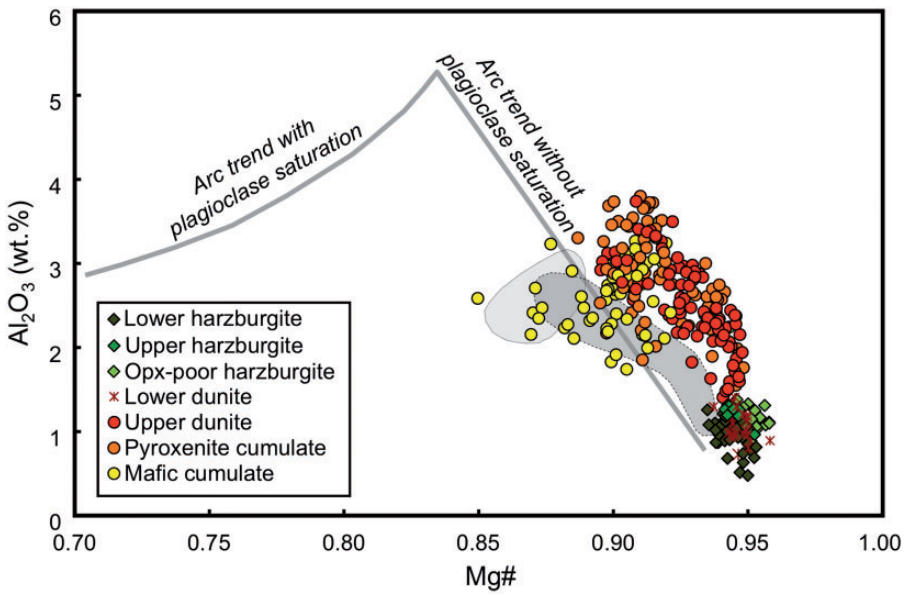

Fig. 15. Al_2O_3 vs Mg# in clinopyroxene of the Massif du Sud. Red and orange circles are crustal cumulates (dunite and pyroxenite) with no obvious plagioclase saturation; yellow circles are gabbronorite with abundant plagioclase. The arc trend is defined for the typical arc cumulates of the Chilas complex, Kohistan (Jagoutz *et al.*, 2007). Fields for Oman wehrlites and gabbronorites (Koepke *et al.*, 2009) without (dark grey) and with (light grey) plagioclase saturation are also shown for comparison with trends from the Massif du Sud.

the peridotites, which is documented in high-temperature shearing of the harzburgite and the presence of melt channels parallel to the foliation. This initial formation stage of the ophiolite is interpreted as a spreading environment, inducing the exhumation of the mantle and associated adiabatic melting. Early work on the origin of the New Caledonia ophiolite argued from both geochemical (Dupuy *et al.*, 1981; Prinzhofer & Allègre, 1985) and

structural (Prinzhofer & Nicolas, 1980; Prinzhofer *et al.*, 1980) evidence that the Massif du Sud was composed of oceanic crust plus underlying mantle formed at the southern flank of a slow-spreading ridge oriented parallel to the Norfolk Ridge (Titus *et al.*, 2011).

However, this early ridge history does not explain the extreme geochemical depletion observed in the peridotites of New Caledonia. The absence of primary clinopyroxene in the harzburgite of the Massif du Sud suggests high amounts of partial melting. Previous whole-rock studies have shown that REE patterns correspond to partial melting of 25–30% (Marchesi *et al.*, 2009; Ulrich *et al.*, 2010). Such high degrees of depletion were initially explained by a disequilibrium model in which melting would occur from depth (garnet facies) to shallow conditions (plagioclase facies) (Prinzhofer & Allègre, 1985). However, it has subsequently been shown that plagioclase peridotite melting is unlikely to occur (Niu, 2004) and we propose that a secondary melting event has occurred in a supra-subduction zone environment.

The position of the peridotites within the olivine–spinel mantle array (Arai, 1994) shows that the entire ultramafic section of New Caledonia preserves a supra-subduction zone signature (Fig. 16). Harzburgites and dunites display values that differ from those of abyssal peridotites (Dick & Bullen, 1984) and the data would suggest that the final melting event occurred between 5 and 10 kbar (Sobolev & Batanova, 1995; Pearce *et al.*, 2000) at 25–30% partial melting (Arai, 1994). This pressure lies in the spinel-facies field for Cr-rich harzburgite (Borghini *et al.*, 2010) and is compatible with the absence of plagioclase in the Massif du Sud. The presence of spinels with high Cr-number and extremely low TiO_2 in a hydrous environment is in agreement with a supra-subduction zone environment (Arai *et al.*, 2006). However, with the exception of some Cr-rich dunites, the Cr-number of spinels is not sufficiently high to be indicative of a source for boninitic lavas and occupies an intermediate position between residues of island arc tholeiites and boninitic melts (Fig. 17). The particular setting of the ophiolite (see below), coupled with the very low amount of TiO_2 in both spinel and clinopyroxene exsolution, suggests that the Massif du Sud might have witnessed the production and the transport of fore-arc basalts to the surface (Fig. 17a) (Reagan *et al.*, 2010). Silicate melts would have been formed during a melting event of the fore-arc mantle, producing chromite pods, hydrous mafic magmas and replacive dunites (Kubo, 2002) and leaving an LREE-enriched residue similar to the peridotites of the Mirdita ophiolite, which were recently characterized as a fore-arc basalt source (Morishita *et al.*, 2011). A secondary fore-arc magmatic event such as the one responsible for refertilization and boninitic magmatism in northern New Caledonia ophiolites (Ulrich *et al.*, 2010) also has to be considered as an influx source for the LREE enrichment, the homogenization of spinel compositions and the further depletion of peridotites in MREE and HREE.

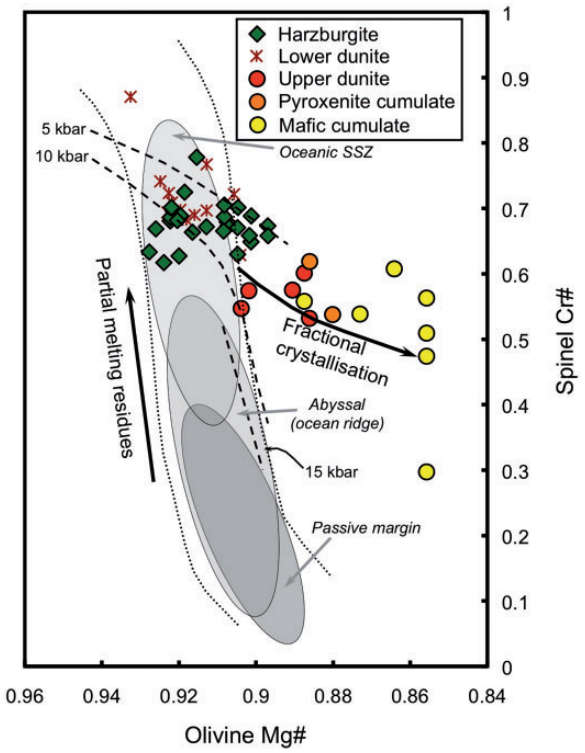

Fig. 16. Average Mg# of olivine and Cr# of spinel in harzburgites, dunites and cumulates from the Massif du Sud. The olivine–spinel mantle array (OSMA) is shown by the two dotted lines. Top light grey ellipse is for supra-subduction peridotites, middle ellipse is the field for abyssal peridotites and the dark grey ellipse covers peridotites recovered in passive margins (Dick & Bullen, 1984; Arai, 1994; Pearce *et al.*, 2000). Pressure curves (dashed lines) give approximate values for the depth of melting of the peridotites. The 5 and 10 kbar curves are from Sobolev & Batanova (1995); the 15 kbar curve is from Jacques & Green (1980). The arrows indicate the residual character in the peridotites and the fractional crystallization trend in the crustal cumulates from cumulate dunite (high Mg#) to gabbronorite (Mg# < 0·88). The distinction between replacive olivine and spinel from the lower dunite (stars) and cumulative dunite (red circles) is clearly visible and confirms that accumulation was the main formation process for the upper dunite.

The discrepancy between pressures estimated for gabbro crystallization (~2–4 kbar) and the last recorded pressure of partial melting for the peridotites (5–10 kbar) suggests that these two events did not occur simultaneously. Gabbro dykes crosscut the upper harzburgite and the dunite zone leading to local metasomatism (Fig. 9). These mafic dykes share similar compositions with the large crustal gabbronorite sills, clearly showing that the intrusion of mafic melt in the lowermost crust is a subsequent event to the main depletion of the harzburgite. Calculated parental melts of the gabbro (Fig. 11) show similarities to boninites (Marchesi *et al.*, 2009), but also have significant depletion in LREE

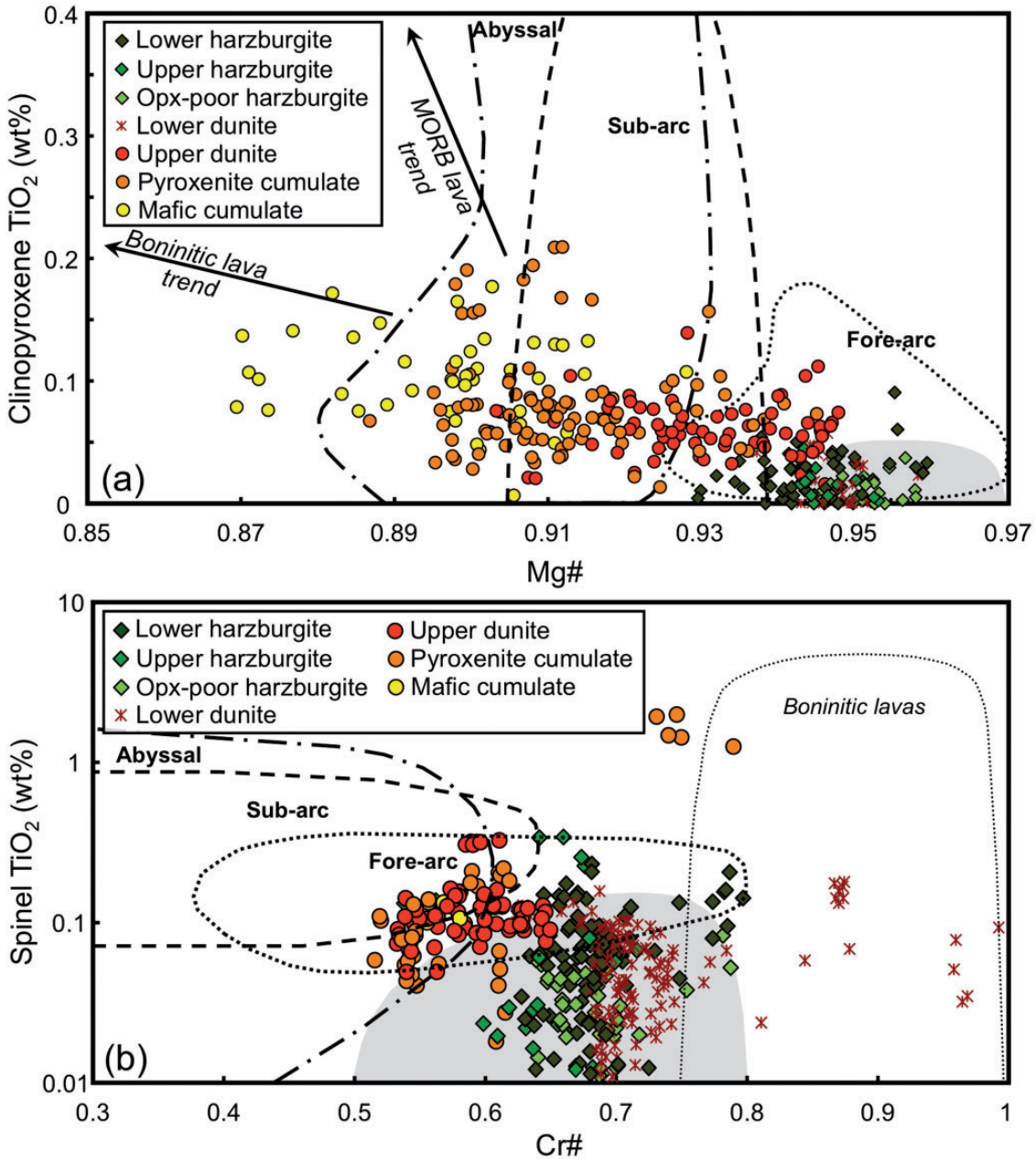

Fig. 17. (a) TiO_2 in clinopyroxene as a function of Mg#. Peridotites show very low TiO_2 contents with high Mg-number and lie in the supra-subduction zone field of Ishii *et al.* (1992) and more particularly mostly in the fore-arc magmatism field (grey zone) of Morishita *et al.* (2011). Sub-arc and abyssal peridotites (Johnson *et al.*, 1990; Brandon & Draper, 1996) generally show higher TiO_2 contents and lower Mg-numbers. Mafic cumulates show a trend with decreasing Mg-number and a very slight increase in TiO_2. General trends for boninitic (Clénet *et al.*, 2010) and MORB lavas (Benoit *et al.*, 1999) are shown for comparison. (b) TiO_2 content vs Cr-number in spinels. Peridotites lie entirely in the fore-arc magmatism field (grey zone) of Morishita *et al.* (2011). Fore-arc, sub-arc and abyssal fields are for spinel peridotites sampled from various environments (Kamenetsky *et al.*, 2001). Spinels from boninite lavas are taken from the Barnes & Roeder (2001) database.

and enrichment in LILE. Such features would suggest that the parental melts of the gabbros had a shallow subduction component (Pearce *et al.*, 2005). The recalculated parental melts have trace element characteristics between those of boninitic melts and primitive arc basalts (Fig. 11).

The low pressure for the crystallization of the mafic sills indicates that this arc-related magmatism in the Massif du Sud ophiolite is more characteristic of a nascent arc. Therefore, substantial differences arise when compared with other exposed arc crust–mantle transition sections

such as Kohistan, where pressures are estimated to be above 10 kbar (Burg *et al.*, 1998).

Implications

Tectonic setting

Our study shows that the Massif du Sud ophiolite evolved from a spreading centre to a convergent margin environment. The increasing amount of information gathered from volcanic arcs, ophiolites and various deep-sea drilling programs has shown in recent decades that MORB oceanic crust is very unlikely to be obducted (Stern, 2004). From the data we collected and previous information on the ultramafic terrane and the Norfolk Ridge, it is thought that the Massif du Sud ophiolite was formed in a suprasubduction setting (Aitchison *et al.*, 1995; Cluzel *et al.*, 2001). Geodynamic reconstructions of the SW Pacific place the New Caledonia ophiolite as the ultra-depleted fore-arc mantle of the Loyalty arc (Eissen *et al.*, 1998; Crawford *et al.*, 2003; Whattam *et al.*, 2008), with the northern lherzolitic massifs as a refertilized mantle wedge (Ulrich *et al.*, 2010). However, the concordance of age between pre-obduction intrusions (Cluzel *et al.*, 2006) in a cold and brittle oceanic crust and the Loyalty arc magmatism (Cluzel *et al.*, 2001) shows that the Massif du Sud oceanic crust was formed well before the Eocene fore-arc setting associated with the Loyalty basin subduction. The geodynamic environment in the late Mesozoic and early Cenozoic suggests that lithospheric extension was dominant during the opening of the Tasman Sea and the retreat of the Chatham subduction zone (Schellart *et al.*, 2006). In such an environment, the initial formation of the Massif du Sud could have been related to the spreading of a marginal basin, followed by the formation of thick oceanic crust in an older subduction zone that is no longer present.

The crust–mantle transition in a nascent arc

The standard definition used to place the crust–mantle transition in the oceanic lithosphere is the change from residual peridotite, defined as mantle, to magmatic cumulates (Benn *et al.*, 1988; Miller & Christensen, 1994). Cumulates are considered to be of crustal affinity whereas replacive rocks are mantle-related. The problem is that away from ophiolite sections accessibly exposed by tectonic emplacement on land, crustal thicknesses and the depths of the crust–mantle transition have been deduced from seismic studies, with the crust–mantle transition identified with the seismic Moho. The exceptionally well-preserved sequence from peridotites to gabbros in the Massif du Sud provides an excellent example showing that the Moho cannot necessarily be taken as the crust–mantle transition in the petrological sense. The petrological definition places the crust–mantle transition in the Massif du Sud at a cryptic discontinuity between the lower and upper dunite zone. Neither the dunite-to-pyroxenite transition, nor the first appearance of gabbros, which are both easily visible in the field, represent a significant change in petrogenetic processes, being simply different lithologies within the cumulate sequence.

The seismic velocities in the Massif du Sud section can be estimated based on previous work. In the Bay of Islands fore-arc ophiolite, a seismic velocity cross-section has been established through the sequence of gabbro, pyroxenite, dunite and harzburgite (V_p 6·85, 7·64, 8·45 and 8·33 km s^{-1} respectively), which form an ophiolitic stratigraphic column similar to that of the Massif du Sud (Salisbury & Christensen, 1978). If we consider the modal composition of depleted harzburgite and dunite in the Massif du Sud ophiolite, P-wave velocities would be $8{\cdot}4 \pm 0{\cdot}2$ and $8{\cdot}5 \pm 0{\cdot}2$ km s^{-1} respectively (Kelemen & Holbrook, 1995). Thus, the distinction between the upper and lower dunite zone and the uppermost peridotites is within the uncertainty of average velocity determination for the mantle (Holbrook *et al.*, 1999). Significantly lower velocities would coincide with the first occurrence of gabbros, which occurs several hundreds of metres above the transition from replacive dunite (uppermost mantle) to cumulus dunite (lowermost crust; Fig. 3). The implication is that seismic studies identifying the Moho with the crust–mantle transition considerably underestimate the extent of partial melting producing arc crust. In the South Loyalty basin, considered as the oceanic equivalent of the Massif du Sud ophiolite, the Moho is interpreted as the crust–mantle transition between gabbro (V_p $6{\cdot}6 \pm 0{\cdot}4$ km s^{-1}) and ultramafic rocks (V_p $8{\cdot}2 \pm 0{\cdot}2$ km s^{-1}), totalling 6·5 km of basaltic crust (Collot *et al.*, 1987), similar to inferred crustal thicknesses at typical mid-ocean ridges (e.g. White *et al.*, 1992). However, this similarity is probably misleading insofar as it neglects the presence of dunite and pyroxenite cumulates as part of the crust.

Although there is no discontinuity in average seismic wave speed in the two types of dunite, which mask the petrological crust–mantle transition, there is a clear difference in fabric between the isotropic cumulates and the strongly sheared rocks of the lower dunite zone. In the Antalya ophiolite, geophysical studies have shown that harzburgite tectonites have up to ΔV_p 3% anisotropy (maximum 9%) and ΔV_s 4% (maximum 10%) (Peselnick & Nicolas, 1978). Such anisotropic behaviour might be detectable and thus there is potential to identify the true crust–mantle boundary on seismic profiles.

The arc crust bulk composition is generally thought to be andesitic, but the primitive arc melts feeding the crust are basaltic, leading to the arc paradox where large amounts of cumulates should lie under the arc to maintain mass balance (Kelemen *et al.*, 2003). The presence of an important ultramafic cumulate pile at the base of the oceanic crust is a key observation to understand this system. Average arc compositions are mainly estimated from seismic profiles and field observations in exhumed arc

sections. Our study shows that even when the ultramafic keel is preserved, it is difficult to accurately determine the thickness and the origin of the dunite zone with these two techniques. Consequently, the bulk arc crust might be more mafic than generally thought.

The mineralogy and geochemistry of the gabbros provide strong evidence that they derive from primitive hydrous basaltic melts with some boninitic affinity in a nascent arc. The morphology of the gabbronorite intrusions (Fig. 3) is not compatible with models involving large magma chambers in the oceanic crust (Smewing, 1981), and the sharp interface between sills and the surrounding cpx–plag dunite is not consistent with a typical infiltration model. In the latter, wehrlites represent the passageway of basaltic melts (Benn *et al.*, 1988) and gabbro sills are the result of the compaction of wehrlitic mushes, leading to the local accumulation of melts (Boudier & Nicolas, 1995; Godard *et al.*, 2000; Marchesi *et al.*, 2009). The presence of olivine with different major and trace element compositions in the gabbronorite argues against the idea that the sills are the result of infiltration where the host phase is entirely consumed (Benoit *et al.*, 1996). Olivine in the gabbronorites has a composition different from the surrounding olivine-rich rocks, whereas other poikilitic silicates have essentially the same composition. The emplacement of sills through injection events owing to permeability barriers (Kelemen *et al.*, 1996) or the episodic compaction of the olivine–melt mush present in the lower dunite zone (Rabinowicz *et al.*, 1987; Clénet *et al.*, 2010) could explain the morphologies observed in some gabbros. The existence of melt-filled fractures, which would episodically feed gabbro sills, is supported in the Massif du Sud and Oman ophiolite, where dykes and sills have been described as branching into each other (Idlefonse *et al.*, 1993).

CONCLUSIONS

The reappraisal of the geology and geochemistry of the Massif du Sud ophiolite of New Caledonia shows that the peridotites represent an extremely depleted mantle with an important dunite zone and a pyroxene-dominated lower crust. The evolution of the harzburgites provides evidence for earlier depletion, presumably by partial melting in an oceanic spreading environment, followed by further melting in an arc environment. Primitive magmas with high water contents and oxygen fugacity were emplaced at relatively low pressure, suggesting that the Massif du Sud ophiolite formed in a nascent arc. The geochemistry of the cumulates shows that the arc-related melts are intermediate between boninites and primitive arc melts, with similarities to fore-arc basalts.

A detailed study of the crust–mantle transition in this nascent arc reveals that the boundary between crustal and mantle material is diffused over a several hundred metres thick dunite zone. With detailed petrography and olivine trace element geochemistry it is possible to subdivide this zone into residual dunites that form the uppermost portion of the mantle and olivine cumulates that represent the lowermost crust. The data presented in this study show that the petrological crust–mantle transition in such an arc environment does not correlate with the increase in V_p from 7 to 8 km s^{-1} (Moho). However, the crust–mantle transition might be imaged using the difference in seismic anisotropy, as the residual dunites are highly deformed whereas the dunite cumulates display a random orientation. The correct location of the crust–mantle transition is necessary for the estimation of the bulk composition of arc crust.

ACKNOWLEDGEMENTS

This study required fieldwork in remote areas of the mountains of New Caledonia. We thank the DIMENC and the DENV for granting us access to high-protection reserves and national parks, and for their help in logistics and guidance. We acknowledge Charlotte Allen and Frances Jenner for assistance with LA-ICP-MS. Carl Spandler is thanked for his careful review of an early version of this paper. We thank Tomo Morishita, Elisabetta Rampone and Oliver Jagoutz for their very constructive reviews.

FUNDING

This project has been financially supported by the Australian Research Council.

SUPPLEMENTARY DATA

Supplementary data for this paper are available at *Journal of Petrology* online.

REFERENCES

Aitchison, J. C., Clarke, G. L., Meffre, S. & Cluzel, D. (1995). Eocene arc–continent collision in New Caledonia and implications for regional southwest Pacific tectonic evolution. *Geology* **23(2)**, 161–164.

Aldanmaz, E., Schmidt, M. W., Gourgaud, A. & Meisel, T. (2009). Mid-ocean ridge and supra-subduction geochemical signatures in spinel-peridotites from the Neothyan ophiolites in SW Turkey: Implications for upper mantle melting processes. *Lithos* **113**, 691–708.

Arai, S. (1994). Characterization of spinel peridotites by olivine–spinel compositional relationships: review and interpretation. *Chemical Geology* **113**, 191–204.

Arai, S. & Ishimaru, S. (2008). Insights into petrological characteristics of the lithosphere of mantle wedge beneath arcs through peridotite xenoliths: a review. *Journal of Petrology* **49(4)**, 665–695.

Arai, S., Kadoshima, K. & Morishita, T. (2006). Widespread arc-related melting in the mantle section of the northern Oman ophiolite as inferred from detrital chromian spinels. *Journal of the Geological Society, London* **163**, 869–879.

Auboin, J., Mattauer, M. & Allègre, C. (1977). La couronne ophiolitique périaustralienne: un charriage oceanique représentatif des stades précoces de l'évolution alpine. *Comptes Rendus de l'Académie des Sciences, Série D* **285**, 953–956.

Augé, T. & Legendre, O. (1994). Platinum-group element oxides from the Pirogues ophiolitic mineralization, New Caledonia: Origin and significance. *Economic Geology* **89**, 1454–1468.

Augé, T. & Maurizot, P. (1995). Stratiform and alluvial platinum mineralization in the New Caledonia ophiolite complex. *Canadian Mineralogist* **33**, 1023–1045.

Augé, T., Cabri, L. J., Legendre, O., McMahon, G. & Cocherie, A. (1999). PGE distribution in base-metals alloys and sulphides of the New Caledonia ophiolite. *Canadian Mineralogist* **37**, 1147–1161.

Barnes, S. J. & Roeder, P. L. (2001). The range of spinel compositions in terrestrial mafic and ultramafic rocks. *Journal of Petrology* **42(12)**, 2279–2302.

Bédard, J. H. & Hébert, R. (1998). Formation of chromitites by assimilation of crustal pyroxenites and gabbros into peridotitic intrusions: North Arm Mountain massif, Bay of Islands ophiolite, Newfoundland, Canada. *Journal of Geophysical Research* **103(B3)**, 5165–5184.

Benn, K., Nicolas, A. & Reuber, I. (1988). Mantle–crust transition zone and origin of wehrlitic magmas: Evidence from the Oman ophiolite. *Tectonophysics* **151**, 75–85.

Benoit, M., Polvé, M. & Ceuleneer, G. (1996). Trace element and isotopic characterization of mafic cumulates in a fossil mantle diapir (Oman ophiolite). *Chemical Geology* **134**, 199–214.

Benoit, M., Ceuleneer, G. & Polvé, M. (1999). The remelting of hydrothermally altered peridotite at mid-ocean ridges by intruding mantle diapirs. *Nature* **402**, 514–518.

Bertrand, P. & Mercier, J.-C. C. (1985). The mutual solubility of coexisting ortho- and clinopyroxene: toward an absolute geothermometer for the natural system? *Earth and Planetary Science Letters* **76**, 109–122.

Blatter, D. L. & Carmichael, I. S. E. (1998). Hornblende peridotite xenoliths from central Mexico reveal the highly oxidized nature of subarc upper mantle. *Geology* **26(11)**, 1035–1038.

Borghini, G., Fumagalli, P. & Rampone, E. (2010). The stability of plagioclase in the upper mantle: subsolidus experiments on fertile and depleted lherzolite. *Journal of Petrology* **51(1–2)**, 229–254.

Boudier, F. & Coleman, R. G. (1981). Cross section through the peridotite in the Semail ophiolite. *Journal of Geophysical Research* **86**, 2573–2592.

Boudier, F. & Nicolas, A. (1995). Nature of the Moho transition zone in the Oman ophiolite. *Journal of Petrology* **36**, 777–796.

Boudier, F., Nicolas, A. & Idlefonse, B. (1996). Magma chambers in the Oman ophiolite: fed from the top and the bottom. *Earth and Planetary Science Letters* **144**, 239–250.

Boudier, F., Godard, M. & Armbruster, C. (2000). Significance of gabbronorite occurrence in the crustal section of the Semail ophiolite. *Marine Geophysical Researches* **21**, 307–326.

Brandon, A. D. & Draper, D. S. (1996). Constraints on the origin of the oxidation state of the mantle overlying subduction zones: an example from Simcoe, Washington, USA. *Geochimica et Cosmochimica Acta* **60**, 1739–1749.

Brey, G. P. & Köhler, T. (1990). Geothermobarometry in four-phase lherzolites II. New thermobarometers, and practical assessment of existing thermobarometers. *Journal of Petrology* **31(6)**, 1353–1378.

BRGM & DIMENC-SGNC. (2001). Carte géologique de Nouvelle Calédonie au 1/200 000. *Mémoire BRGM* **113**, 279.

Burg, J.-P., Bodinier, J.-L., Chaudhry, S., Hussain, S. & Dawwod, H. (1998). Infra-arc mantle–crust transition and intra-arc mantle diapirs in the Kohistan Complex (Pakistani Himalaya): petrostructural evidence. *Terra Nova* **10(2)**, 74–80.

Cassard, D., Nicolas, A., Rabinowicz, M., Moutte, J., Leblanc, M. & Prinzhofer, A. (1981). Structural classification of chromite pods in Southerm New Caledonia. *Economic Geology* **76**, 805–831.

Clénet, H., Ceuleneer, G., Pinet, P., Abily, B., Daydou, Y., Harris, E., Amri, I. & Dantas, C. (2010). Thick sections of layered ultramafic cumulates in the Oman ophiolite revealed by an airborne hyperspectral survey: Petrogenesis and relationship to mantle diapirism. *Lithos* **114**, 265–281.

Clift, P. D., Pavlis, T., DeBari, S. M., Draut, A.E., Rioux., M. & Kelemen, P. B. (2005). Subduction érosion of the Jurassic Talkeetna–Bonanza arc and the Mesozoic accretionary tectonics of western North America. *Geology* **33**, 881–884.

Cluzel, D. & Meffre, S. (2002). L'unité de la Boghen (Nouvelle-Calédonie, Pacifique sud-ouest): un complexe d'accrétion jurassique. Données radiochronologies préliminaires U–Pb sur les zircons détritiques. *Comptes Rendus de l'Académie des Sciences—Géoscience* **334**, 867–875.

Cluzel, D., Chiron, D. & Courme, M.-D. (1998). Discordance de l'Eocène supérieur et événements pré-obduction en Nouvelle-Calédonie. *Comptes Rendus de l'Académie des Sciences—Sciences de la Terre et des Planètes* **327**, 485–491.

Cluzel, D., Aitchison, J. C. & Picard, C. (2001). Tectonic accretion and underplating of mafic terranes in the Late Eocene intraoceanic fore-arc of New Caledonia (Southwest Pacific): geodynamic implications. *Tectonophysics* **340(1–2)**, 23–60.

Cluzel, D., Bosch, D., Paquette, J.-L., Lemennicier, Y., Montjoie, P. & Ménot, R.-P. (2005). Late Oligocene post-obduction granitoids of New Caledonia: A case for reactivated subduction and slab breakoff. *Island Arc* **14**, 254–271.

Cluzel, D., Meffre, S., Maurizot, P. & Crawford, A. J. (2006). Earliest Eocene (53 Ma) convergence in the Southwest Pacific: evidence from pre-obduction dikes in the ophiolite of New Caledonia. *Terra Nova* **18**, 395–402.

Cluzel, D., Jourdan, F., Meffre, S., Maurizot, P. & Lesimple, S. (2012). The metamorphic sole of New Caledonia ophiolite; $^{40}Ar/^{39}Ar$, U–Pb, and geochemical evidence for subduction inception at a spreading ridge. *Tectonics*, **31(3)**, TC3016.

Coleman, R. G. (1977). *Ophiolites: Ancient Oceanic Lithosphere?* Berlin: Spinger, 229 p.

Collot, J.-Y., Malahoff, A., Récy, J., Latham, G. & Missègue, F. (1987). Overthrust emplacement of New Caledonia ophiolite: geophysical evidence. *Tectonics* **6**, 215–232.

Coogan, L. A., Banks, G. J., Gillis, K. M., MacLeod, C. J. & Pearce, J. A. (2003). Hidden melting signatures recorded in the Troodos ophiolite plutonic suite: evidence for widespread generation of depleted melts and intra-crustal melt aggregation. *Contributions to Mineralogy and Petrology* **144**, 484–505.

Crawford, A. J., Meffre, S. & Symonds, P. A. (2003). 120 to 0 Ma tectonic evolution of the southwest Pacific and analogous geological evolution of the 600 to 220 Ma Tasman Fold Belt System, In: Hillis, R.R. & Muller, R.D. (eds) *Evolution and Dynamics of the Australian Plate. Geological Society of America, Special Papers* **372**, 383–403.

DeBari, S. M. & Coleman, R. G. (1989). Examination of the deep levels of an island arc: evidence from the Tonsina ultramafic–mafic assemblage, Tonsina, Alaska. *Journal of Geophysical Research* **94(B4)**, 4373–4391.

Dhuime, B., Bosch, D., Bodinier, J.-L., Garrido, C. J., Brugiuer, O., Hussain, S. S. & Dawood, H. (2007). Multistage evolution of the Jilal ultramafic–mafic complex (Kohistan, N.Pakistan): Implications for building the root of island arcs. *Earth and Planetary Science Letters* **261**, 179–200.

Dick, H. J. B. & Bullen, T. (1984). Chromian spinel as a petrogenetic indicator in abyssal and alpine type peridotites and spatially associated lavas. *Contributions to Mineralogy and Petrology* **86**, 54–76.

Dilek, Y., Furnes, H. & Shallo, M. (2007). Suprasubduction zone ophiolite formation along the periphery of Mesozoic Gondwana. *Gondwana Research*, doi:10.1016/j.gr.2007.01.005.

Dupuy, C., Dostal, J. & Leblanc, M. (1981). Geochemistry of an ophiolitic complex from New Caledonia. *Contributions to Mineralogy and Petrology* **76**, 77–83.

Eggins, S. M., Kinsley, L. P. J. & Shelley, J. M. G. (1998). Deposition and element fractionation processes during atmospheric pressure laser sampling for analysis by ICP-MS. *Applied Surface Science* **129**, 278–286.

Eissen, J.-P., Crawford, A. J., Cotton, J., Meffre, S., Bellon, H. & Delaune, M. (1998). Geochemistry and tectonic significance of basalts in the Poya terrane, New Caledonia. *Tectonophysics* **284**, 203–219.

Elthon, D., Casey, J. F. & Komor, S. (1982). Mineral chemistry of ultramafic cumulates from the North Arm mountain massif of the Bay of Islands ophiolite: evidence for high-pressure crystal fractionation of oceanic basalts. *Journal of Geophysical Research* **87**, 8717–8734.

Fabries, J. (1979). Spinel–olivine geothermometry in peridotite from ultramafic complexes. *Contributions to Mineralogy and Petrology* **69**, 329–336.

Feig, S. T., Koepke, J. & Snow, J. E. (2006). Effect of water on tholeiitic basalt phase equilibria: an experimental study under oxidizing conditions. *Contributions for Mineralogy and Petrology* **152**, 611–638.

Field, S. W. & Haggerty, S. E. (1994). Symplectites in upper mantle peridotites: development and implications for the growth of subsolidus garnet, pyroxene and spinel. *Contributions to Mineralogy and Petrology* **118**, 138–156.

Fitzherbert, J. A., Clarke, G. L. & Powell, R. (2003). Lawsonite–omphacite-bearing metabasites of the Pam Peninsula, NE New Caledonia: Evidence for disrupted blueschist- to eclogite-facies conditions. *Journal of Petrology* **44**, 1805–1831.

Gaetani, G. A., Grove, T. L. & Bryan, W. B. (1993). The influence of water on the petrogenesis of subduction-related igneous rocks. *Nature* **365**, 332–334.

Garrido, C. J., Bodinier, J.-L., Burg, J.-P., Zeilinger, G., Hussain, S. S., Dawood, H., Chaudry, M. N. & Gervilla, F. (2006). Petrogenesis of mafic garnet granulite in the lower crust of the Kohistan paleo-arc complex (Northern Pakistan): Implications for intra-crustal differentiation of island arcs and generation of continental crust. *Journal of Petrology* **47(10)**, 1873–1914.

Garrido, C. J., Bodinier, J.-L., Dhuime, B., Bosch, D., Chanefo, I., Bruguier, O., Hussain, S. S., Dawood, H. & Burg, J.-P. (2007). Origin of the island-arc Moho transition zone via melt–rock reactions and its implication for intracrustal differentiation of island arcs: Evidence from the Jilal complex (Kohistan complex, northern Pakistan). *Geology* **35**, 683–686.

Gasparik, T. (1984). Two-pyroxene thermobarometry with new experimental data in the system $CaO–MgO–Al_2O_3–SiO_2$. *Contributions to Mineralogy and Petrology* **87**, 87–97.

George, R. P. (1978). Structural petrology of the Olympus ultramafic complex in the Troodos ophiolite, Cyprus. *Geological Society of America Bulletin* **89**, 845–865.

Girardeau, J. & Nicolas, A. (1981). Structures in two of the Bay of Islands (Newfoundland) ophiolite massifs: a model for oceanic crust and upper mantle. *Tectonophysics* **77**, 1–34.

Godard, M., Jousselin, D. & Bodinier, J.-L. (2000). Relationships between geochemistry and the structure beneath a palaeo-spreading centre: a study of the mantle section in the Oman ophiolite. *Earth and Planetary Science Letters* **180**, 133–148.

Grove, T. L. & Baker, M. B. (1984). Phase equilibrium controls on the tholeiitic versus calc-alkaline differentiation trends. *Journal of Geophysical Research* **89**, 3253–3274.

Guillon, J. H. (1975). Les massifs péridotitiques de Nouvelle-Calédonie. Type d'appareil ultrabasique stratiforme de chaine récente. *ORSTOM Mémoires* **76**, 120.

Guillon, J. H. & Lawrence, L. J. (1973). The opaque minerals of the ultramafic rocks of New Caledonia. *Mineralium Deposita* **8**, 115–126.

Hauri, E. H., Wagner, T. P. & Grove, T. L. (1994). Experimental and natural partitioning of Th, U, Pb and other trace elements between garnet, clinopyroxene and basaltic melts. *Chemical Geology* **117**, 149–166.

Herzberg, C. T. (1978). Pyroxene geothermometry and geobarometry: experimental and thermodynamic evaluation of some subsolidus phase relations involving pyroxenes in the system $CaO–MgO–Al_2O_3–SiO_2$. *Geochimica et Cosmochimica Acta* **42**, 945–957.

Hirschmann, M. M. & Stolper, E. M. (1996). A possible role for garnet pyroxenite in the origin of the garnet signature in MORB. *Contributions to Mineralogy and Petrology* **124**, 185–208.

Holbrook, W. S., Lizarralde, D., McGeary, S., Bangs, N. & Diebold, J. (1999). Structure and composition of the Aleutian island arc and implications for continental crustal growth. *Geology* **27**, 31–34.

Holloway, J. R. & Burnham, C. W. (1972). Melting relations of basalt with equilibrium water pressure less than total pressure. *Journal of Petrology* **13**, 1–29.

Idlefonse, B., Nicolas, A. & Boudier, F. (1993). Evidence from the Oman ophiolite for sudden stress changes during melt injection at oceanic spreading centres. *Nature* **366**, 673–675.

Ishii, T., Robinson, P. T., Mackawa, H. & Fiske, R. (1992). Petrological studies of peridotites from diapiric serpentinite seamounts in the Izu–Ogazawara–Marianas forearc. Leg 125. *Proceedings of the Ocean Drilling Program, Scientific Results* **125**, 445–485.

Jacques, A. L. & Green, D. H. (1980). Anhydrous melting of peridotite at 0–15 kb pressure and the genesis of tholeiitic basalts. *Contributions to Mineralogy and Petrology* **73**, 287–310.

Jagoutz, O., Müntener, O., Ulmer, P., Pettke, T., Burg, J.-P., Dawood, H. & Hussain, S. (2007). Petrology and mineral chemistry of lower crustal intrusions: the Chilas Complex, Kohistan (NW Pakistan). *Journal of Petrology* **48(10)**, 1895–1953.

Jenner, F. E. & O'Neill, H. St. C. (2012). Analysis of 60 elements in 616 ocean floor basaltic glasses. *Geochemistry, Geophysics, Geosystems* **13**, Q02005, doi:10.1029/2011GC004009.

Johnson, K. T. M., Dick, H. J. B. & Shimizu, N. (1990). Melting in the oceanic upper mantle: an ion microprobe study of diopsides in abyssal peridotites. *Journal of Geophysical Research* **95**, 2661–2678.

Jousselin, D. & Nicolas, A. (2000). The Moho transition zone in the Oman ophiolite—relation with wehrlites in the crust and dunites in the mantle. *Marine Geophysical Researches* **21**, 229–241.

Juster, T. C., Grove, T. L. & Perfit, M. R. (1989). Experimental constraints on the generation of Fe–Ti basalts, andesites, and rhyodacites at the Galapagos spreading centre, 85°W and 95°W. *Journal of Geophysical Research* **94**, 9251–9274.

Kamenetsky, V. S., Crawford, A. J. & Meffre, S. (2001). Factors controlling chemistry of magmatic spinel: an empirical study of associated olivine, Cr-spinel and melt inclusions from primitive rocks. *Journal of Petrology* **42(4)**, 655–671.

Kelemen, P. B. & Holbrook, W. S. (1995). Origin of thick, high-velocity igneous crust along the U.S. East coast margin. *Journal of Geophysical Research* **100(B7)**, 10077–10094.

Kelemen, P. B., Johnson, K. T. M., Kinzler, R. J. & Irving, A. J. (1990). High field strength element depletions in arc basalts due to mantle–magma interactions. *Nature* **345**, 521–524.

Kelemen, P. B., Koga, K. & Shimizu, N. (1996). Geochemistry of gabbro sills in the crust–mantle transition zone of the Oman ophiolite: implications for the origin of the oceanic lower crust. *Earth and Planetary Science Letters* **146**, 475–488.

Kelemen, P. B., Hanghøj, K. & Greene, A. R. (2003). One view of the geochemistry of subduction-related magmatic arcs, with emphasis on primitve andesite and lower crust. In: Rudnick, R. L. (ed.) *Geochemistry of the Crust. Treatise on Geochemistry, Vol. 3.* Oxford: Elsevier–Pergamon, pp. 593–659.

Keller, N., Arculus, R. J., Hermann, J. & Richards, S. (2008). Submarine back-arc lava with arc signature; Fonulafei center, northeast Lau Basin, Tonga. *Journal of Geophysical Research* **113(B8)**, B08S07.

Koepke, J., Schoenborn, S., Oelze, M., Wittmann, H., Feig, S. T., Hellebrand, E., Boudier, F. & Schoenberg, R. (2009). Petrogenesis of crustal wehrlites in the Oman ophiolite: Experiments and natural rocks. *Geochemistry, Geophysics, Geosystems* **10(10)**, 26. p.

Köhler, T. P. & Brey, G. P. (1990). Calcium exchange between olivine and clinopyroxene calibrated as a geothermobarometer for natural peridotites from 2 to 60 kb with applications. *Geochimica et Cosmochimica Acta* **54**, 2375–2388.

Kubo, K. (2002). Dunite formation processes in highly depleted peridotite: Case study of the Iwanaidake peridotite, Hokkaido, Japan. *Journal of Petrology* **43(3)**, 423–448.

Lippard, S. J., Shelton, A. W. & Gass, I. G. (eds) (1986). *The Ophiolite of Northern Oman. Geological Society, London, Memoirs* **11**, 178 p.

Mallmann, G. & O'Neill, H. St. C. (2009). The crystal/melt partitioning of V during mantle melting as a function of oxygen fugacity compared with some other elements (Al, P, Ca, Sc, Ti, Cr, Fe, Ga, Y, Zr and Nb). *Journal of Petrology* **50(9)**, 1765–1794.

Marchesi, C., Garrido, C. J., Godard, M., Belley, F. & Ferré, E. (2009). Migration and accumulation of ultra-depleted subduction-related melts in the Massif du Sud ophiolite (New Caledonia). *Chemical Geology* **266**, 180–195.

McDonough, W. F. & Sun, S. (1995). The composition of the Earth. *Chemical Geology* **120**, 223–253.

McKenzie, D. & Bickle, M. J. (1988). The volume and composition of melt generated by extension of the lithosphere. *Journal of Petrology* **29**, 625–679.

McPherson, E., Thirlwall, M. F., Parkinson, I. J., Menzies, M. A., Bodinier, J.-L., Woodland, A. & Bussod, G. (1996). Geochemistry of metasomatism adjacent to amphibole-bearing veins in the Lherz peridotite massif. *Chemical Geology* **134**, 135–157.

Mercier, J. C. & Nicolas, A. (1975). Textures and fabrics of upper-mantle peridotites as illustrated by xenoliths from basalts. *Journal of Petrology* **16**, 454–487.

Metcalf, R. V. & Shervais, J. W. (2008). Suprasubduction-zone ophiolites: Is there really an ophiolite conundrum? In: Wright, J. E. & Shervais, J. W. (eds) *Ophiolites, Arcs and Batholiths: A Tribute to Cliff Hopson Geological Society of America, Special Papers* **438**, 191–222.

Miller, D. J. & Christensen, N. I. (1994). Seismic signature and geochemistry of an island arc: A multidisciplinary study of the Kohistan accreted terrane, northern Pakistan. *Journal of Geophysical Research* **99B**, 11623–11642.

Morishita, T., Arai, S. & Green, D. H. (2003). Evolution of low-Al orthopyroxene in the Horoman peridotite, Japan: an unusual indicator of metasomatizing fluids. *Journal of Petrology* **44(7)**, 1237–1246.

Morishita, T., Dilek, Y., Shallo, M., Tamura, A. & Arai, S. (2011). Insight into the uppermost mantle section of a maturing arc: The Eastern Mirdita ophiolite, Albania. *Lithos* **124(3–4)**, 215–226.

Müntener, O., Kelemen, P. B. & Grove, T. L. (2001). The role of H_2O during crystallization of primitive arc magmas under uppermost mantle conditions and genesis of igneous pyroxenites: an experimental study. *Contributions to Mineralogy and Petrology* **141**, 643–658.

Nicolas, A. (1989). *Structures of Ophiolites and Dynamics of Oceanic Lithosphere*. Dordrecht: Kluwer, 368 p.

Nicolas, A. & Prinzhofer, A. (1983). Cumulative or residual origin for the transition zone in ophiolites: structural evidence. *Journal of Petrology* **24**, 188–206.

Nicolas, A., Boudier, F., Cassard, D., Girardeau, J., Prinzhofer, A. & Violette, J. F. (1981). The dunite transition zone in ophiolites mantle partially melted by magma leaking rather than ultramafic cumulate. *Terra Cognita, Special Issue*, A18.

Niu, Y. (2004). Bulk-rock major and trace element compositions of abyssal peridotites: implications for mantle melting extraction and post-melting processes beneath mid-ocean ridges. *Journal of Petrology* **45**, 2423–2458.

O'Neill, H. St. C. (1981). The transition between spinel lherzolite and garnet lherzolite, and its use as a geobarometer. *Contributions to Mineralogy and Petrology* **77**, 185–194.

O'Neill, H. St. C. & Wall, V. J. (1987). The olivine–orthopyroxene–spinel oxygen geobarometer, the nickel precipitation curve, and the oxygen fugacity of the Earth's upper mantle. *Journal of Petrology* **28(6)**, 1169–1191.

Pallister, J. S. & Hopson, C. A. (1981). Samail ophiolite plutonic suite: field relations, phase variation, cryptic variation and layering, and a model of a spreading ridge magma chamber. *Journal of Geophysical Research* **86(B4)**, 2593–2644.

Paris, J.-P. (1981). *Géologie de la Nouvelle Calédonie. Un essai de synthèse. BRGM Mémoire* **113**, 279.

Paris, J.-P. & Lille, R. (1977). La Nouvelle Calédonie du Permien au Miocène. Données cartographiques, hypothèses géotectoniques. Symposium International de Géodynamiques du Sud-Ouest Pacifique, Nouméa, 1976. *Bulletin du BRGM* **4(1)**, 79–95.

Parkinson, I. J. & Arculus, R. J. (1999). The redox state of subduction zones: insights from arc-peridotites. *Chemical Geology* **160**, 409–423.

Pearce, J. A., Stern, R. J., Bloomer, S. H. & Fryer, P. (2005). Geochemical mapping of the Mariana arc–basin system: Implications for the nature and distribution of subduction components. *Geochemistry, Geophysics, Geosystems* **6(7)**, 27. p.

Pearce, J. A., Barker, P. F., Edwards, S. J., Parkinson, I. J. & Leat, P. T. (2000). Geochemistry and tectonic significance of peridotites from the South Sandwich arc–basin system, South Atlantic. *Contributions to Mineralogy and Petrology* **139**, 36–53.

Pearce, N. J. G., Perkins, W. T., Westgate, J. A., Gorton, M. P., Jackson, S. E., Neal, C. B. & Chenery, S. P. (1997). A compilation of new and published major and trace element data for NIST SRM 610 and NIST SRM 612 glass reference materials. *Geostandards News* **21**, 115–144.

Peselnick, L. & Nicolas, A. (1978). Seismic anisotropy in an ophiolite peridotite: Application to oceanic upper mantle. *Journal of Geophysical Research* **83**, 1227–1235.

Picard, C., Audet, M., Goulet, N., Keller, F. & Nicholson, K. (2004). The New Caledonian ophiolite: origin in the South Loyalty Basin (SW Pacific). *EOS Transactions, American Geophysical Union* **85(28)**, Western Pacific geophysical meeting supplementary abstract V23B-97.

Potel, S., Ferreire Mählmann, R., Stern, W., Mullis, J. & Frey, M. (2006). Very low-grade metamorphism evolution of pelitic rocks under high-pressure/low temperature conditions. NW New Caledonia (SW Pacific). *Journal of Petrology* **47**, 991–1015.

Prinzhofer, A. & Allègre, C. J. (1985). Residual peridotites and the mechanisms of partial melting. *Earth and Planetary Science Letters* **74**, 251–265.

Prinzhofer, A. & Nicolas, A. (1980). The Bogota peninsula, New Caledonia, a possible oceanic transform fault. *Journal of Geology* **88**, 387–398.

Prinzhofer, A., Nicolas, A., Cassard, D., Moutte, J., Leblanc, M., Paris, J.-P. & Rabinovitch, M. (1980). Structures in the New Caledonia peridotites–gabbros: Implications for oceanic mantle and crust. *Tectonophysics* **69**, 85–112.

Rabinowicz, M., Ceuleneer, G. & Nicolas, A. (1987). Melt segregation and flow in the mantle diapirs below spreading centers: evidence from Oman ophiolites. *Journal of Geophysical Research* **92**, 3475–3486.

Rampone, E., Vissers, R. L. M., Poggio, M., Scambelluri, M. & Zanetti, A. (2010). Melt migration and intrusion during exhumation of the Alboran lithosphere: the Tallante mantle xenolith record (Betic Cordillera, SE Spain). *Journal of Petrology* **51(1–2)**, 295–325.

Reagan, M. K., Ishizuka, O., Stern, R. J. *et al.* (2010). Fore-arc basalts and subduction initiation in the Izu–Bonin–Mariana system. *Geochemistry, Geophysics, Geosystems* **11(3)**, 17.

Rodgers, K. A. (1975). Lower Tertiary tholeiitic basalts from Southern New Caledonia. *Mineralogical Magazine* **40**, 25–32.

Roeder, P. L., Campbell, I. H. & Jamieson, H. E. (1979). A re-evaluation of the olivine–spinel geothermometer. *Contributions to Mineralogy and Petrology* **68**, 325–334.

Ross, J. V., Mercier, J.-C. C., Ave Lallemant, H. G., Carter, N. L. & Zimmerman, J. (1980). The Vourinos ophiolite complex, Greece: the tectonite suite. *Tectonophysics* **70**, 63–83.

Saccani, E. & Photiades, A. (2004). Mid-ocean ridge and supra-subduction affinities in the Pindos ophiolites (Greece): implications for magma genesis in a forearc setting. *Lithos* **73**, 229–253.

Salisbury, M. H. & Christensen, N. I. (1978). The seismic velocity structure of a traverse through the Bay of Islands Ophiolite complex, Newfoundland, an exporsure of oceanic crust and upper mantle. *Journal of Geophysical Research* **83(B2)**, 805–817.

Schellart, W. P., Lister, G. S. & Toy, V. G. (2006). A late Cretaceous and Cenozoic reconstruction of the Southwest Pacific region: Tectonics controlled by subduction and slab rollback processes. *Earth-Science Reviews* **76**, 191–233.

Sevin, B., Ricordel-Prognon, C., Quesnel, F., Cluzel, D., Lesimple, S. & Maurizot, P. (2011). First palaeomagnetic dating of ferricrete in New Caledonia: new insights on the morphogenesis and palaeoweathering of 'Grande Terre'. *Terra Nova* **24**, 77–85.

Shimizu, Y., Arai, S., Morishita, T. & Ishida, Y. (2008). Origin and significance of spinel–pyroxene symplectite in lherzolite xenoliths from Tallante, SE Spain. *Mineralogy and Petrology* **94**, 27–43.

Sinton, J. J. (1977). Equilibration history of the basal Alpine-type peridotite, Red Mountain, New Zealand. *Journal of Petrology* **18**, 216–246.

Smewing, J. D. (1981). Mixing characteristics and compositional differences in mantle-derived melts beneath spreading axes: Evidence from cyclically layered rocks in the ophiolite of North Oman. *Journal of Geophysical Research* **86B**, 2645–2659.

Smewing, J. D., Christensen, N. I., Bartholemew, I. D. & Browning, P. (1984). The structure of the oceanic upper mantle and lower crust as deduced from the northern section of the Oman ophiolite. In: Gass, I. G., Lippard, S. J. & Shelton, A. W. (eds) *Ophiolites and Oceanic Lithosphere. Geological Society, London, Special Publications* **14**, 41–54.

Sobolev, A. V. & Batanova, V. G. (1995). Mantle lherzolites of the Troodos ophiolite complex, Cyprus: clinopyroxene geochemistry. *Petrology* **3**, 440–448.

Sobolev, A. V. & Danyushevsky, L.V. (1994). Petrology and geochemistry of boninites from the North Termination of the Tonga trench: constraints on the generation conditions of primary High-Ca boninite magmas. *Journal of Petrology* **35(5)**, 1183–1211.

Spandler, C., Rubatto, D. & Hermann, J. (2005). Late Cretaceous–Tertiary tectonics of the southwest Pacific: Insights from U–Pb sensitive, high-resolution ion microprobe (SHRIMP) dating of eclogite facies rocks from New Caledonia. *Tectonics* **24**, TC3003, 16 pp.

Stern, R. J. (2004). Subduction initiation: spontaneous and induced. *Earth and Planetary Science Letters* **226**, 275–292.

Streckeisen, A. (1976). To each plutonic rock its proper name. *Earth-Science Reviews* **12**, 1–33.

Tahirkheli, R. A. K. (1979). Geology of Kohistan and adjoining Eurasian and Indo-Pakistan continents, Pakistan. *Geological Bulletin, University of Peshawar, Special Issue* **11**, 1–30.

Takashima, R., Nishi, H. & Yoshida, T. (2002). Geology, petrology and tectonic setting of the Late Jurassic ophiolite in Hokkaido, Japan. *Journal of Asian Earth Sciences* **21**, 197–215.

Takazawa, E., Okayasu, T. & Satoh, K. (2003). Geochemistry and origin of the basal lherzolites from the northern Oman ophiolite (northern Fizh block). *Geochemistry, Geophysics, Geosystems* **4**, 2.

Titus, S. J., Maes, S. M., Benford, B., Ferré, E. C. & Tikoff, B. (2011). Fabric development in the mantle section of a paleo-transform fault and its effect on ophiolite obduction, New Caledonia. *Lithosphere* **3(3)**, 221–244.

Ulrich, M., Picard, C., Guillot, S., Chauvel, C., Cluzel, D. & Meffre, S. (2010). Multistage melting stages and refertilization as indicators for ridge to subduction formation: The New Caledonia ophiolite. *Lithos* **115**, 223–236.

Varfalvy, V., Hébert, R., Bédard, J. H. & Laflèche, M. R. (1997). Petrology and geochemistry of pyroxenite dykes in upper mantle peridotites of the North Arm Mountain massif, Bay of Islands ophiolite, Newfoundland: Implications for the genesis of boninitic and related magmas. *Canadian Mineralogist* **35**, 543–570.

Violette, J. F. (1980). Structure des ophiolites des Philippines (Zambalès et Palawan) et de Chypre. Ecoulement asthénosphérique sous les zones d'expansion océanique. PhD thesis, University of Nantes.

Wells, P.R.A. (1977). Pyroxene thermometry in simple and complex systems. *Contributions to Mineralogy and Petrology* **62**, 129–139.

Whattam, S. A., Malpas, J., Ali, J. R. & Smith, I. E. M. (2008). New SW Pacific tectonic model: Cyclical intraoceanic magmatic arc construction and near-coeval emplacement along the Australia–Pacific margin in the Cenozoic. *Geochemistry, Geophysics, Geosystems* **9(3)**, Q03021.

White, R. S., McKenzie, D. & O'Nions, R. K. (1992). Oceanic crustal thickness from seismic measurements and rare earth elements inversions. *Journal of Geophysical Research* **97B**, 19683–19715.

Witt-Eickschen, G. & O'Neill, H. St. C. (2005). The effect of temperature on the equilibrium distribution of trace elements between clinopyroxene, orthopyroxene, olivine and spinel in upper mantle peridotite. *Chemical Geology* **221**, 65–101.

Yamasaki, T., Maeda, J. & Mizuta, T. (2006). Geochemical evidence in clinopyroxenes from gabbroic sequence for two distinct magmatisms in the Oman ophiolite. *Earth and Planetary Science Letters* **251**, 52–65.

Yumul, G. (2004). Zambales ophiolite complex (Philippines) transition-zone dunites: Restite, cumulate, or replacive products? *International Geology Review* **46(3)**, 259–272.

Zack, T., Foley, S. F. & Jenner, G. A. (1997). A consistent partition coefficient set for clinopyroxene, amphibole and garnet from laser ablation microprobe analysis of garnet pyroxenites from Kakanui, New Zealand. *Neues Jahrbuch für Mineralogie, Abhandlungen* **172**, 23–41.

Zhou, M.-F., Robinson, P. T., Malpas, J., Edwards, S. J. & Qi, L. (2005). REE and PGE geochemical constraints on the formation of dunites in the Luobusa ophiolite, southern Tibet. *Journal of Petrology* **46(3)**, 615–639.